

## Development of geochemical sensors for continuous, on-line monitoring and modelling of coastal groundwater aquifers

Thorn, Paul

*Publication date:*  
2010

*Document Version*  
Publisher's PDF, also known as Version of record

*Citation for published version (APA):*  
Thorn, P. (2010). *Development of geochemical sensors for continuous, on-line monitoring and modelling of coastal groundwater aquifers*. Roskilde Universitet.

### General rights

Copyright and moral rights for the publications made accessible in the public portal are retained by the authors and/or other copyright owners and it is a condition of accessing publications that users recognise and abide by the legal requirements associated with these rights.

- Users may download and print one copy of any publication from the public portal for the purpose of private study or research.
- You may not further distribute the material or use it for any profit-making activity or commercial gain.
- You may freely distribute the URL identifying the publication in the public portal.

### Take down policy

If you believe that this document breaches copyright please contact [rucforsk@kb.dk](mailto:rucforsk@kb.dk) providing details, and we will remove access to the work immediately and investigate your claim.

# **Appendix A and B**

to the Ph.D. Dissertation:

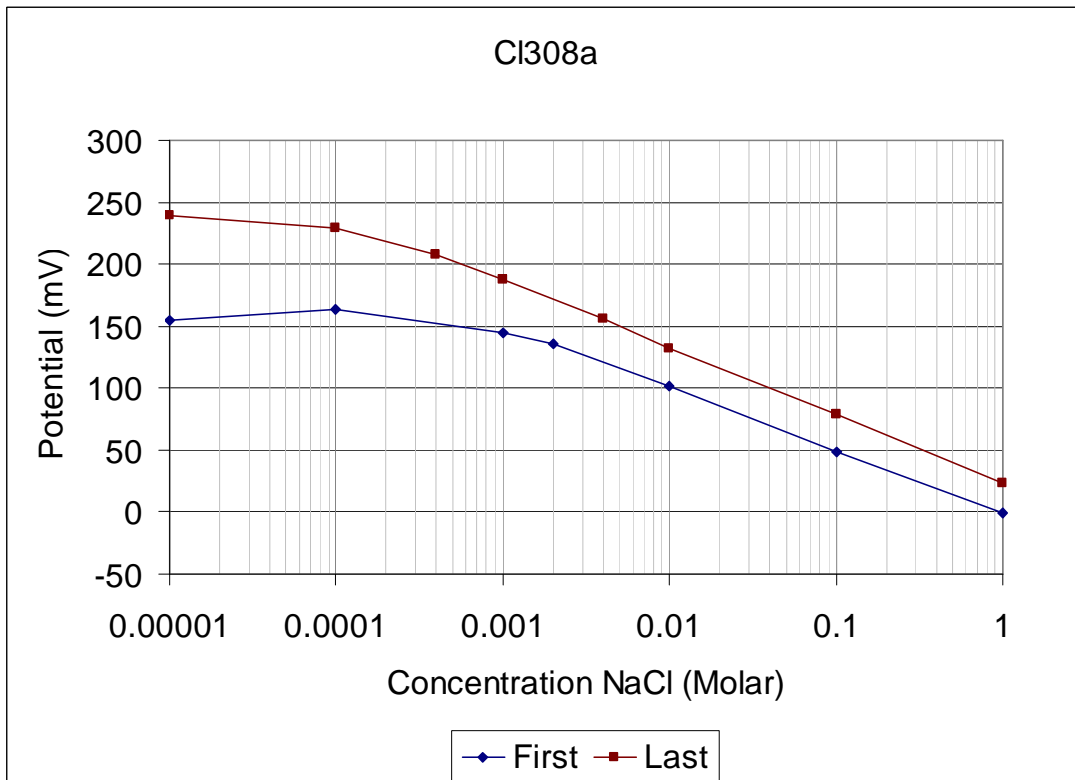
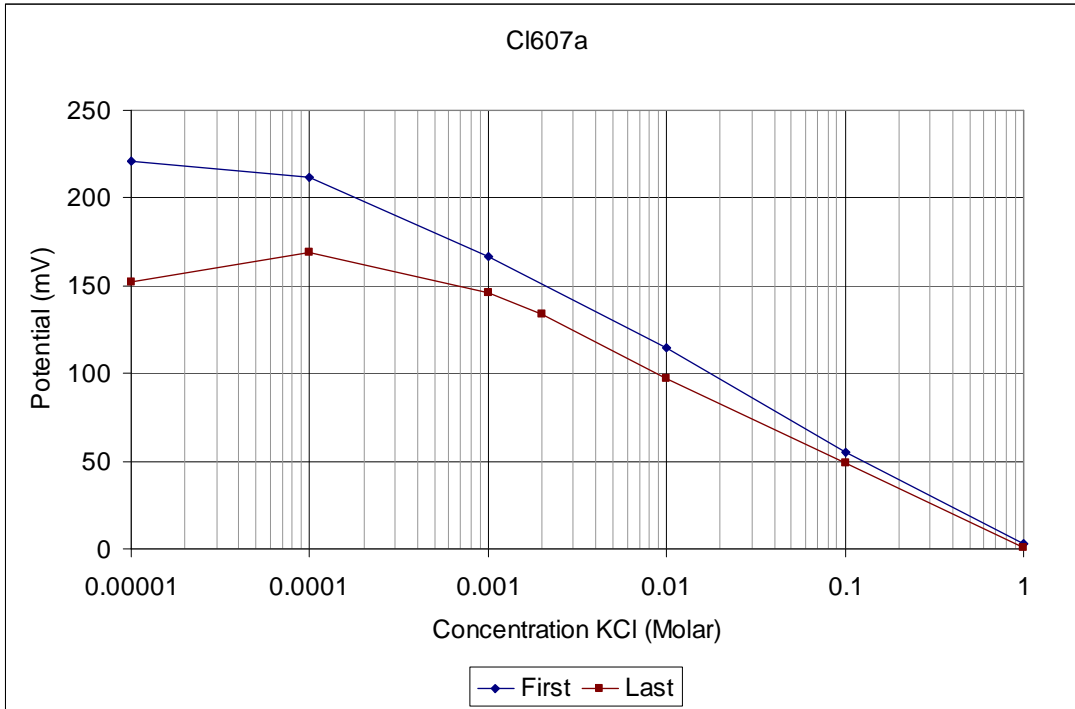
*Development of geochemical sensors for continuous,  
on-line monitoring and modelling of coastal  
groundwater aquifers*

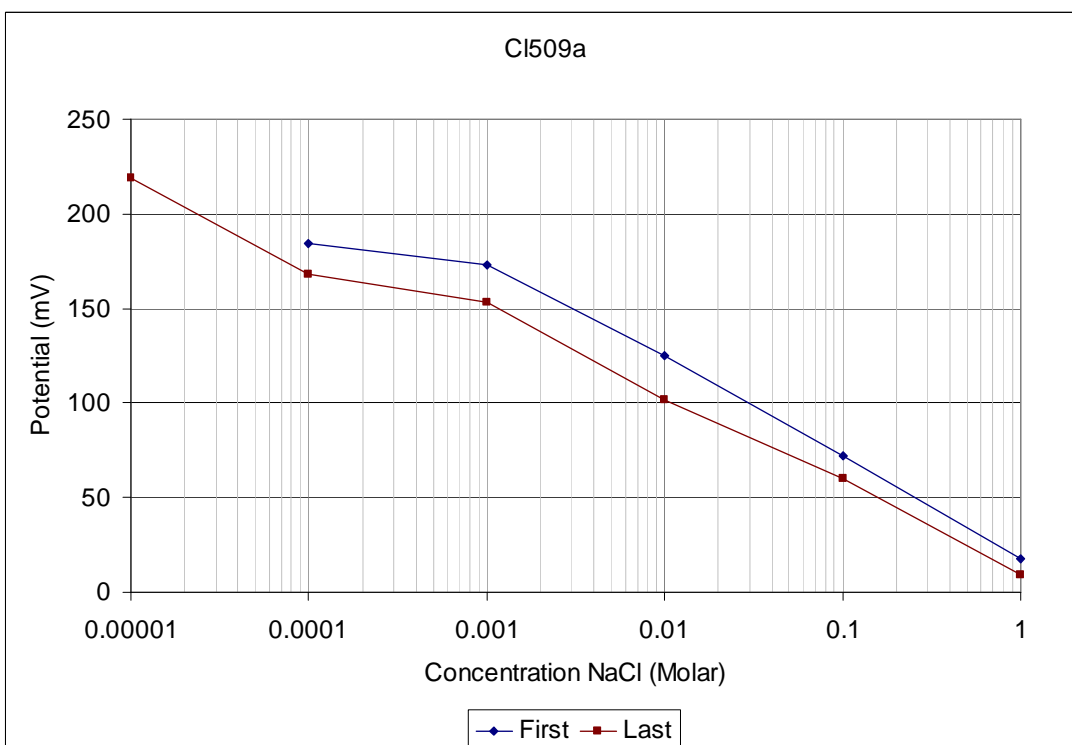
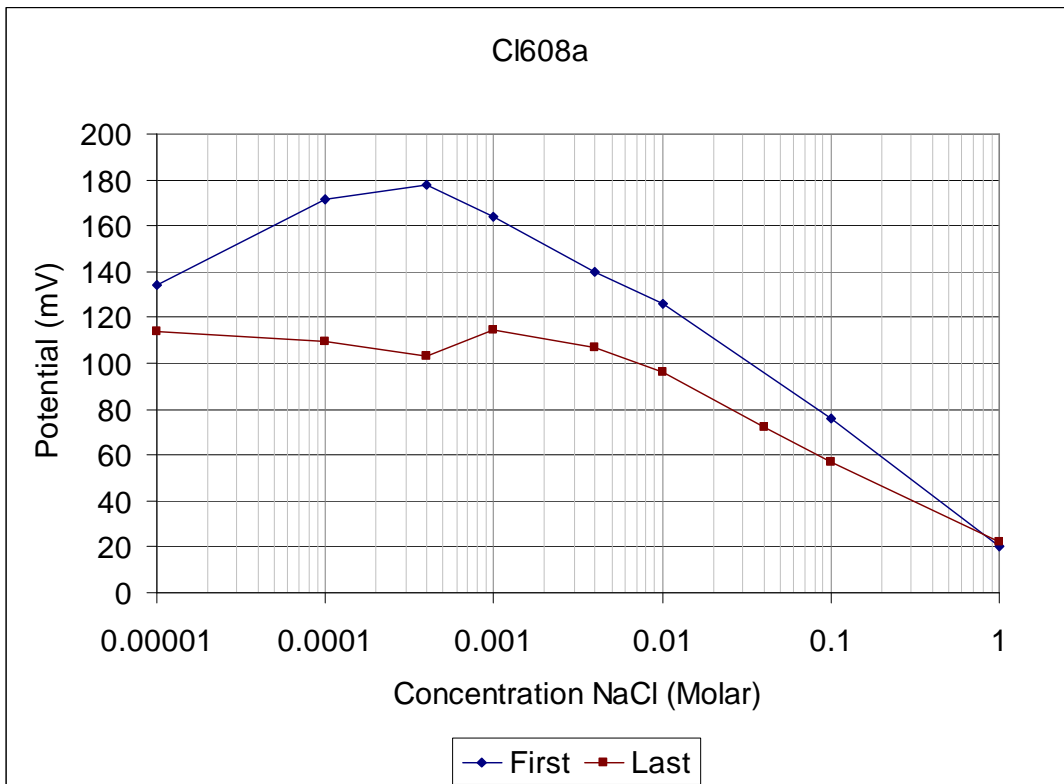
Paul Thorn  
Roskilde University

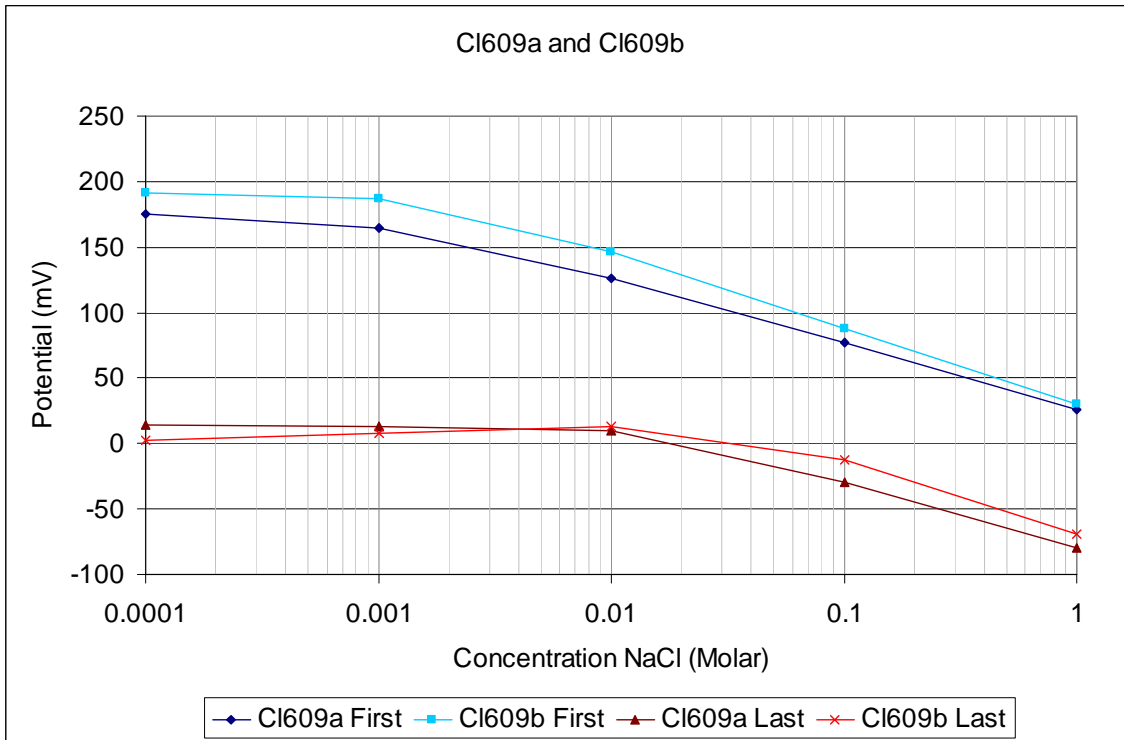
June, 2010

## Appendix A Chloride Sensor Data

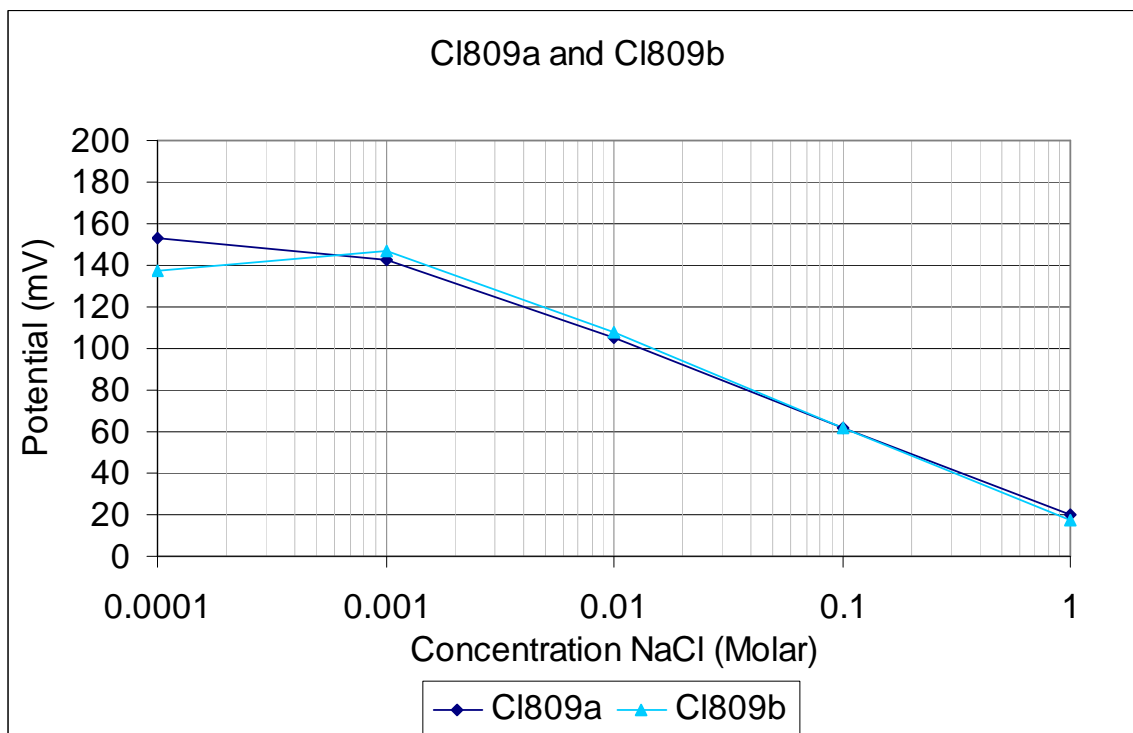
A1. Calibration data, as associated with Table 1 in Chapter 3.



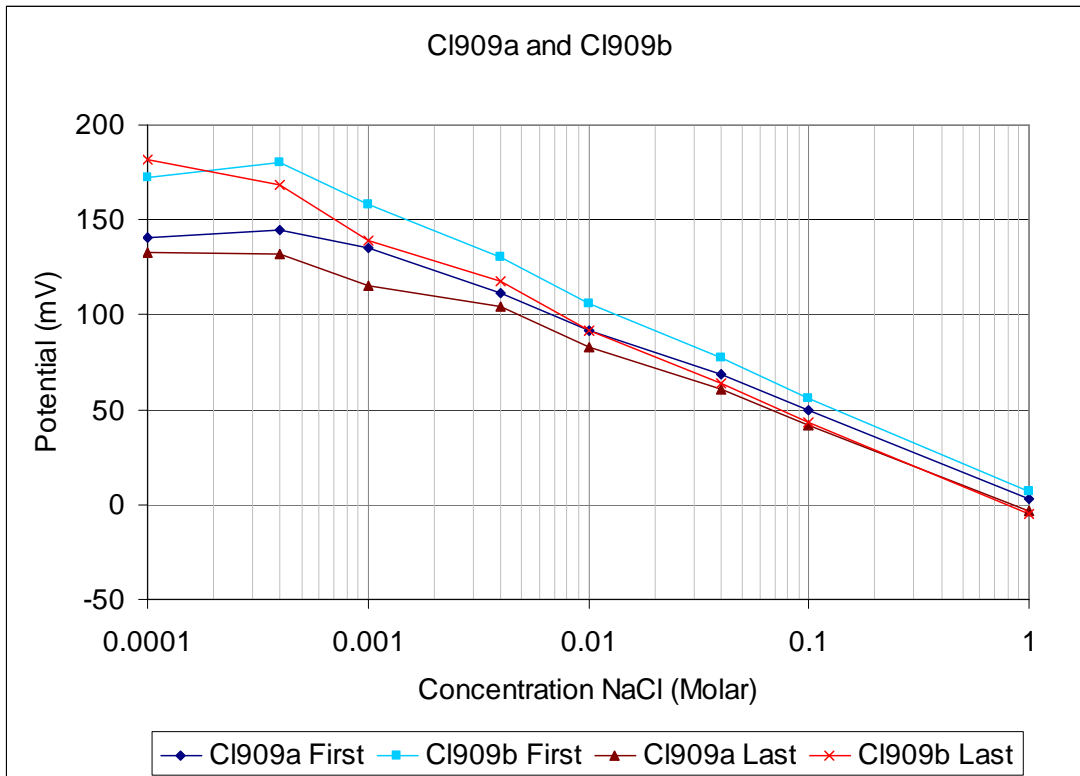




Note: the last measurements conducted on this sensor was after the June/July test in the Greve monitoring well, where the sensors were covered with a bright orange layer of ochre.

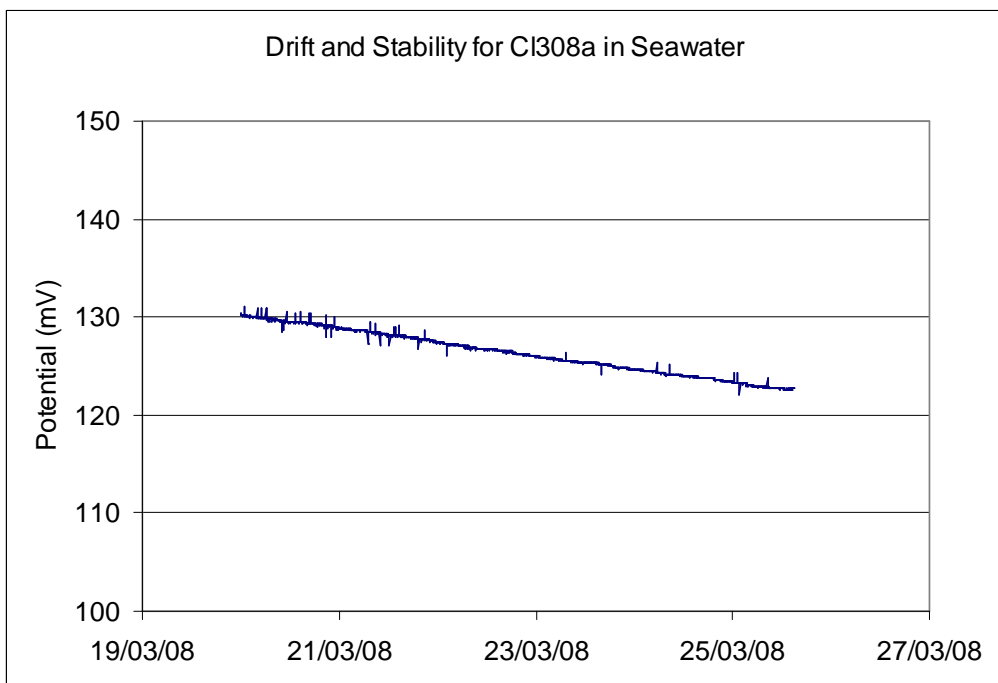
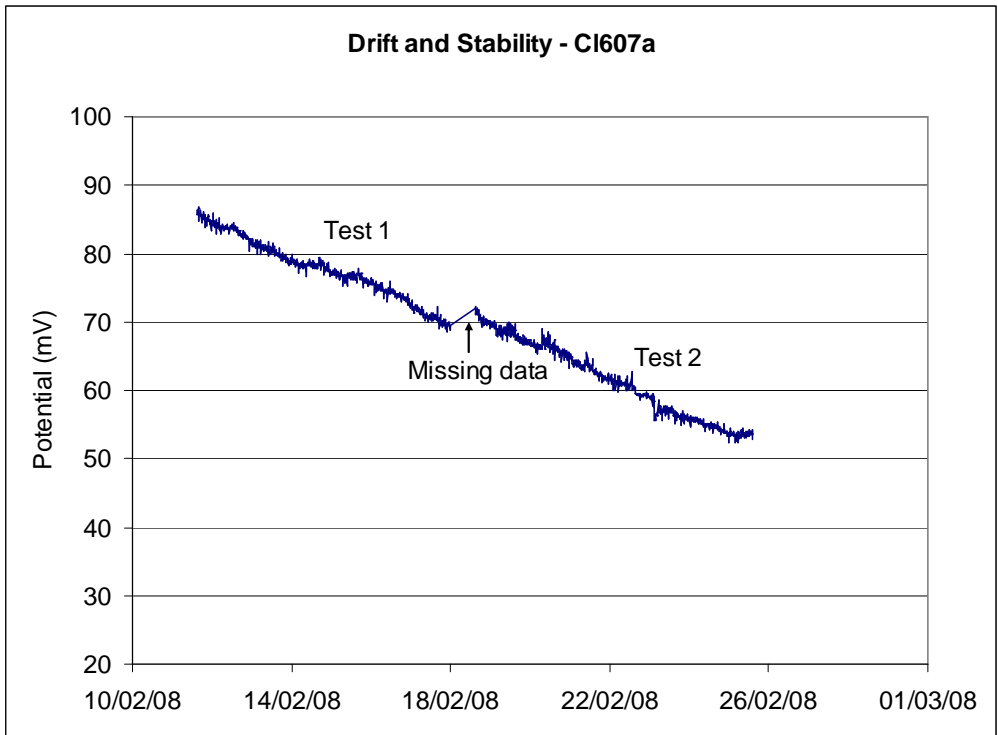


Note: the sensors were used in the August and September Greve monitoring well tests, and no post-test calibration was conducted for these sensors.

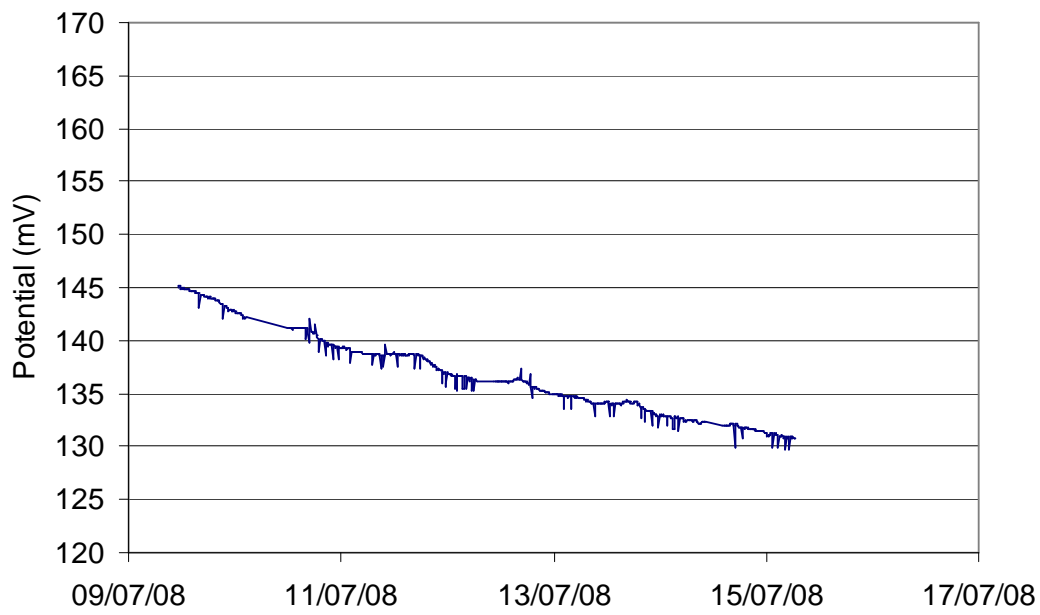


*Note: the measurements show the calibration before the sensors were used in the Wickford monitoring test, and then show the last measurement taken for the sensors.*

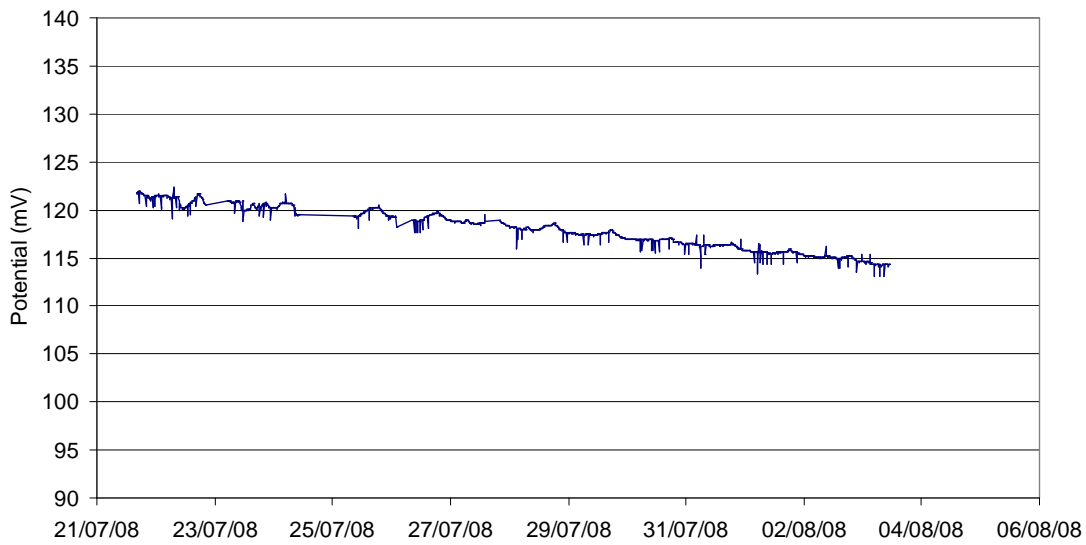
A2. Plots of laboratory tests conducted on the chloride sensors, corresponding to the tests listed in Table 2 of Chapter 3.



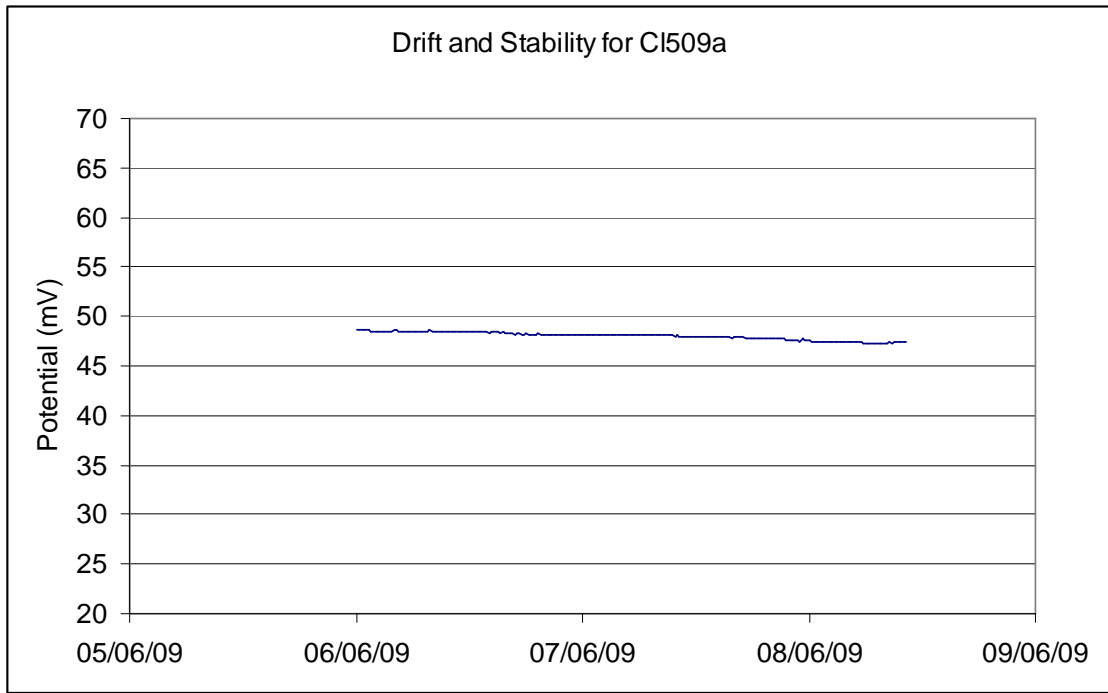
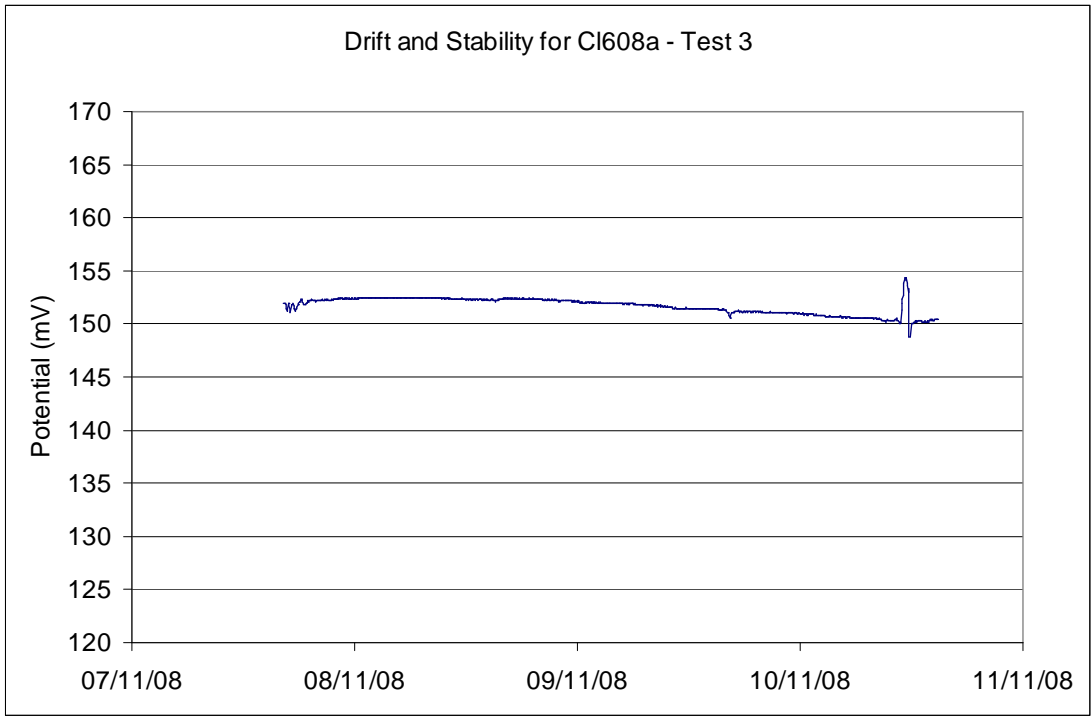
Stability and Drift for Sensor CI608a - Test 1



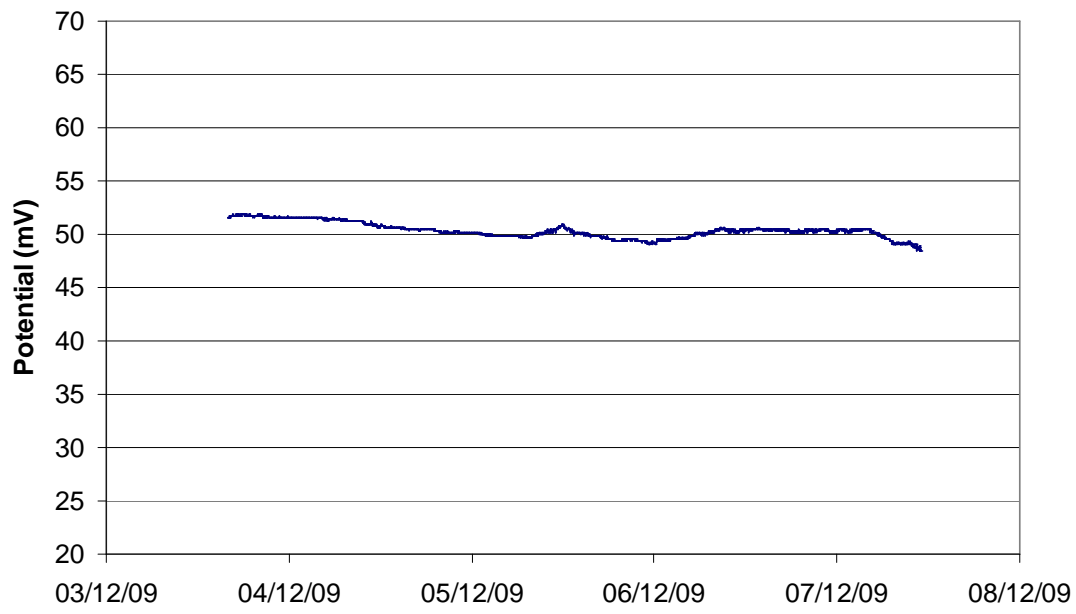
Drift and Stability for CI608a - Test 2







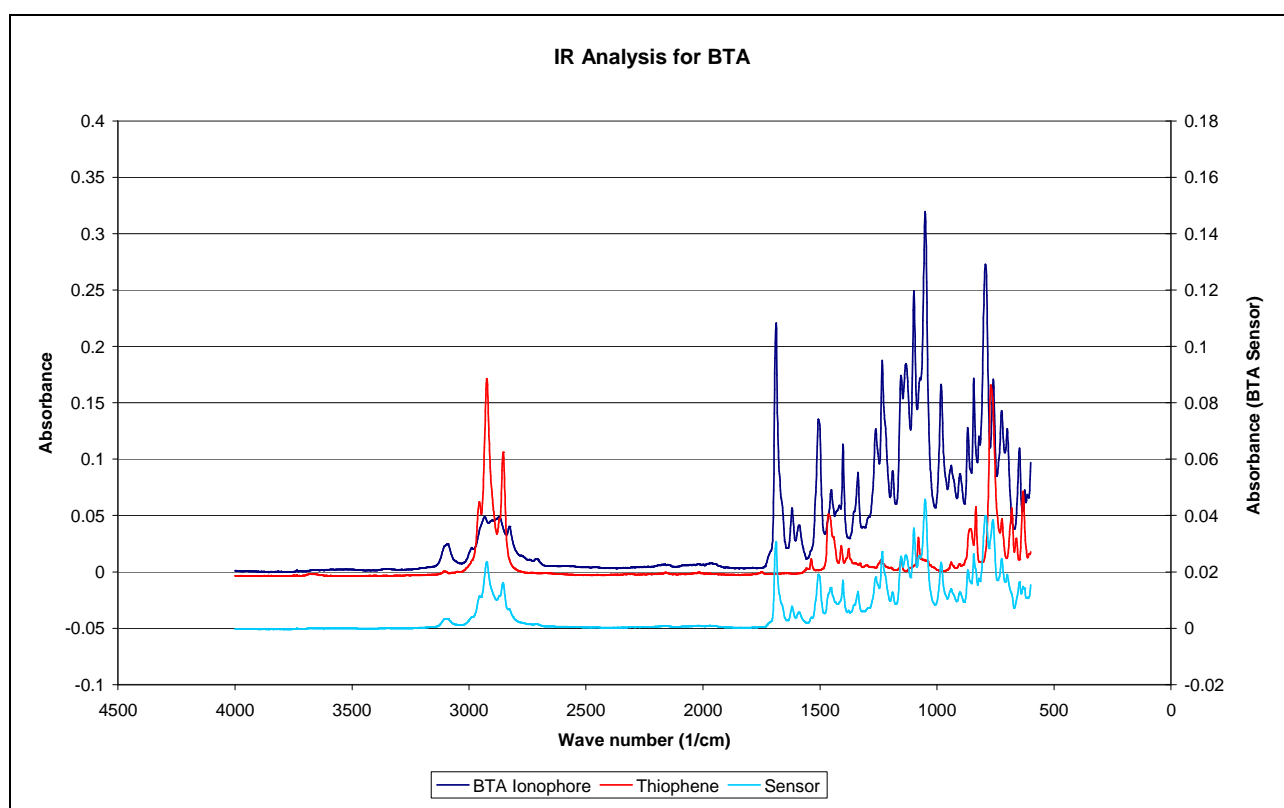
### Drift and Stability - CI909a



## Appendix B Sodium Sensor Data

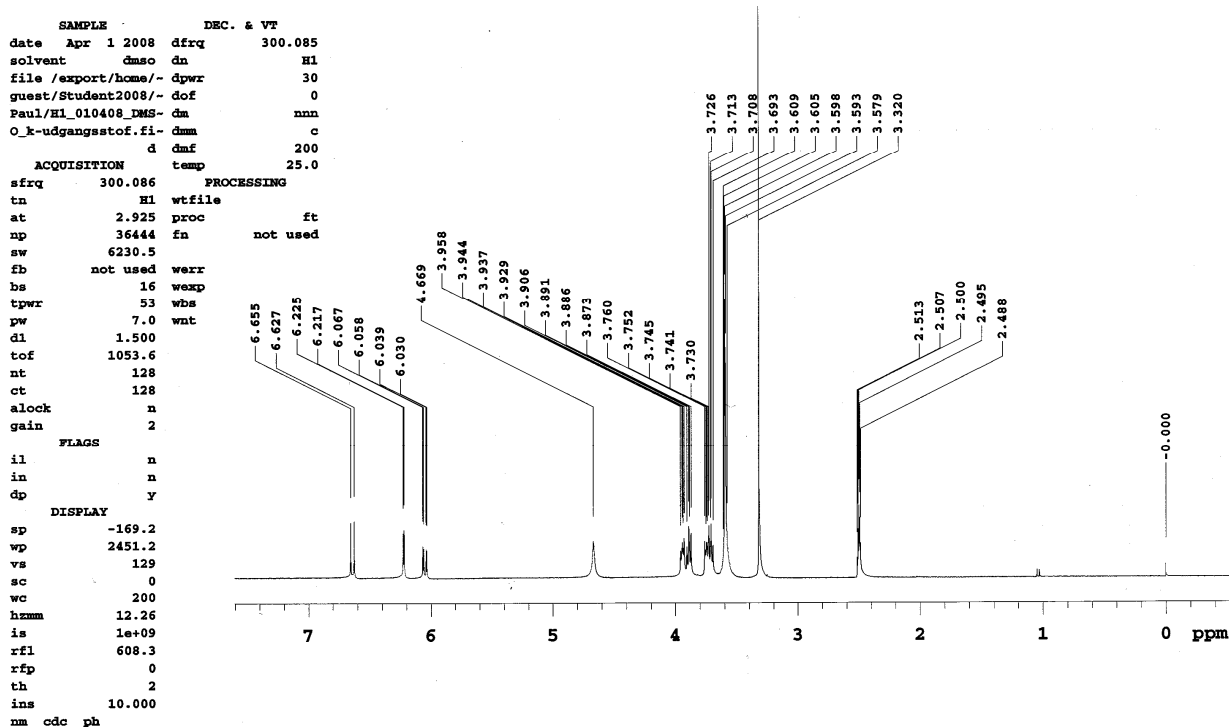
### B1. BTA Sensor Series

#### B1.1 –Infrared absorbance data for the BTA sensors.

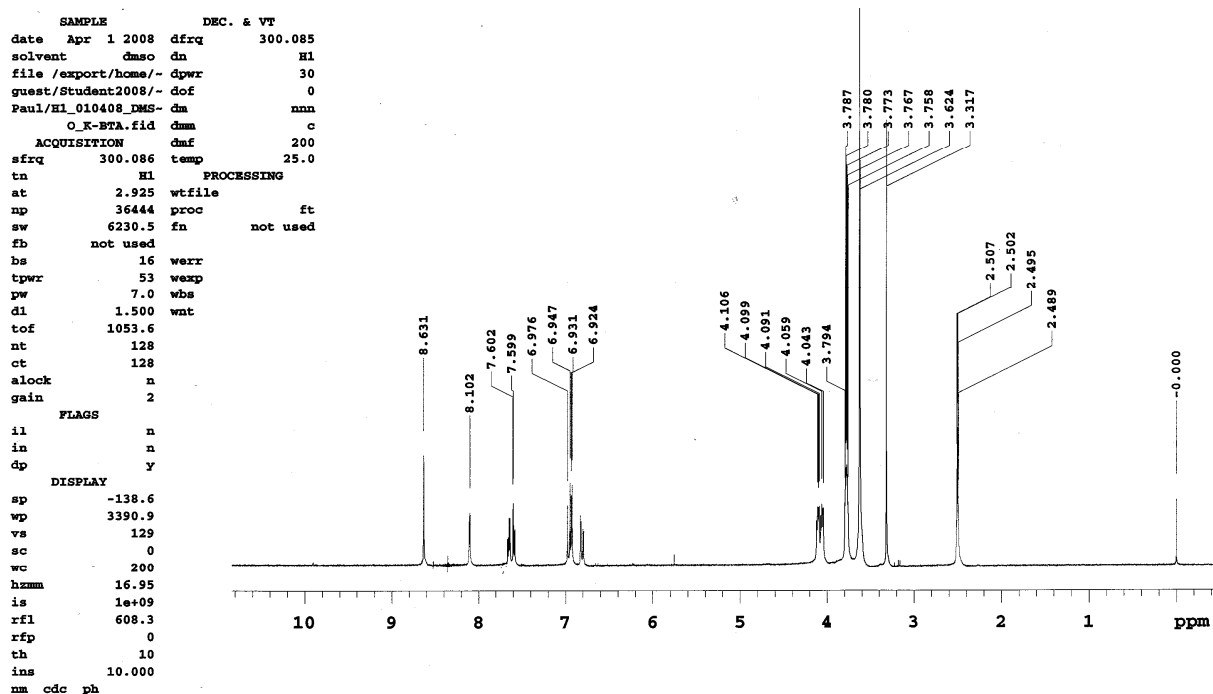


*Infrared absorbance data for the BTA sensor (light blue), where the ionophore and thiophene has been co-polymerized on the gold electrode. For reference, there is also infrared absorbance data for the ionophore (dark blue) and thiophene (red) before polymerisation. From the data, it is apparent that the sensor has predominately the signal of the BTA ionophore, indicating that the ionophore was successfully attached to the gold surface.*

## B1.2 – NMR data for the BTA sensors.

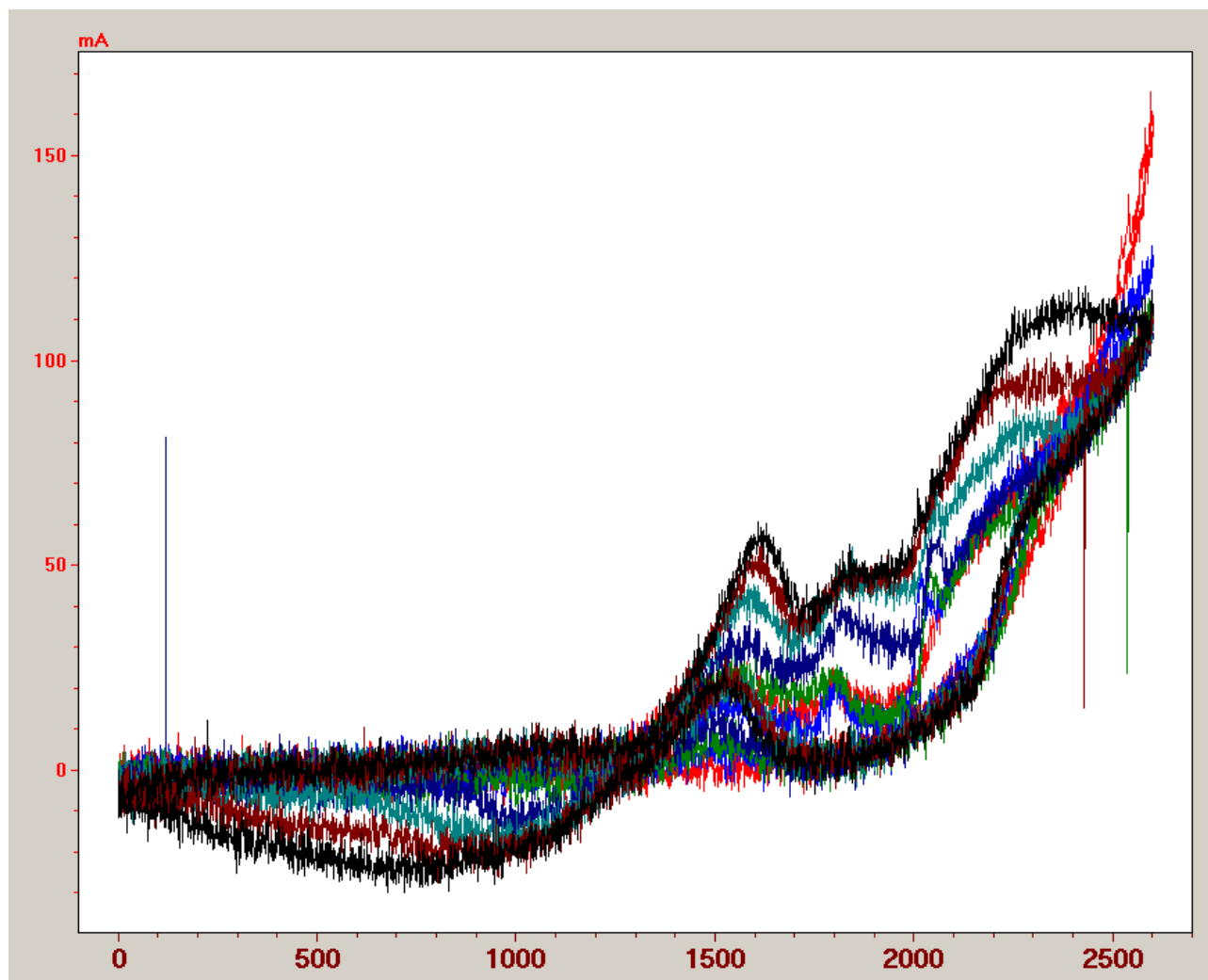


*NMR spectra of the original reagent, 4-aminobenzo-15-crown-5, before the cobbling of the thiophene group to form the BTA ionophore.*



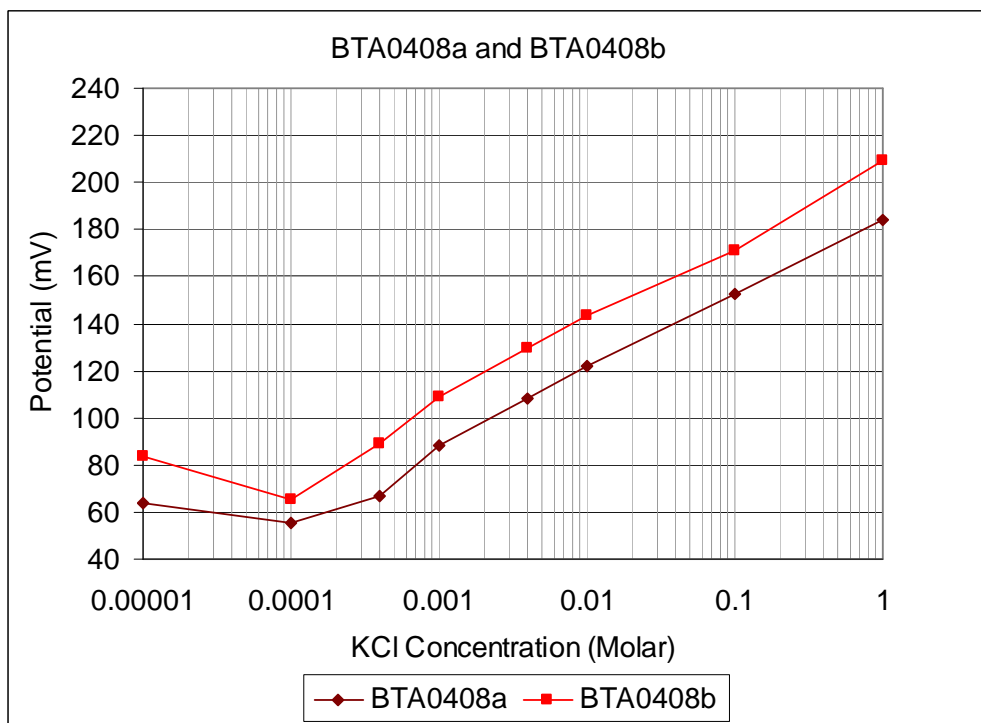
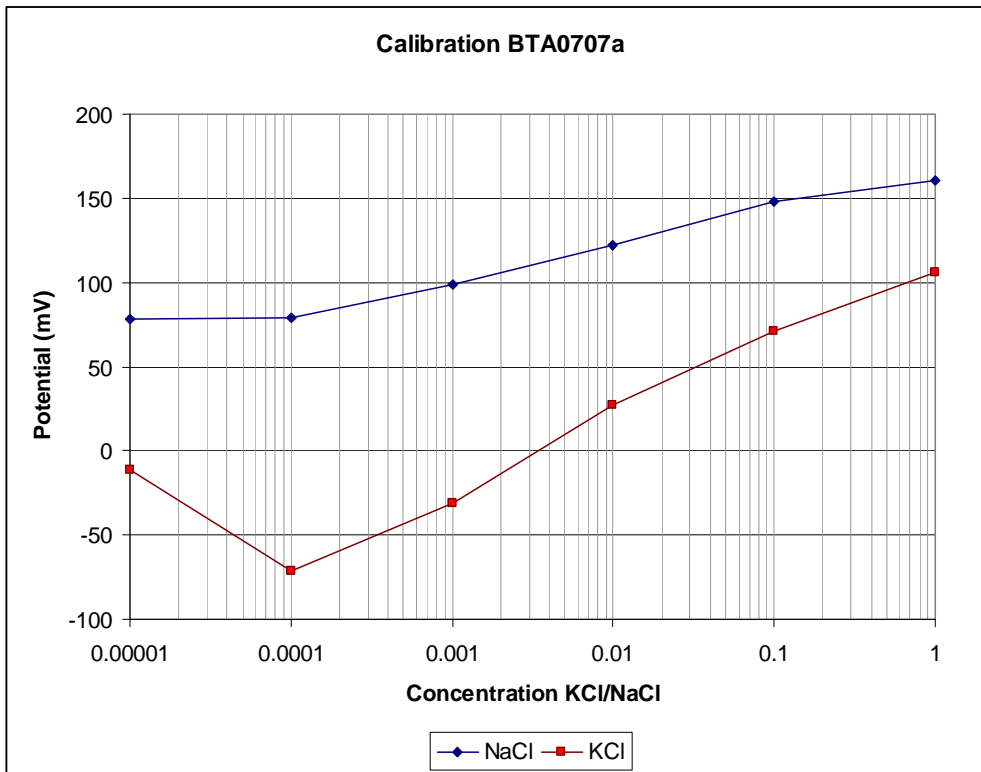
*NMR spectra of the BTA ionophore. Note how the hydrogen peaks from the original reagent moved from between 6 and 7ppm to between 6.9 and 7.8ppm, showing that the reaction went to completion.*

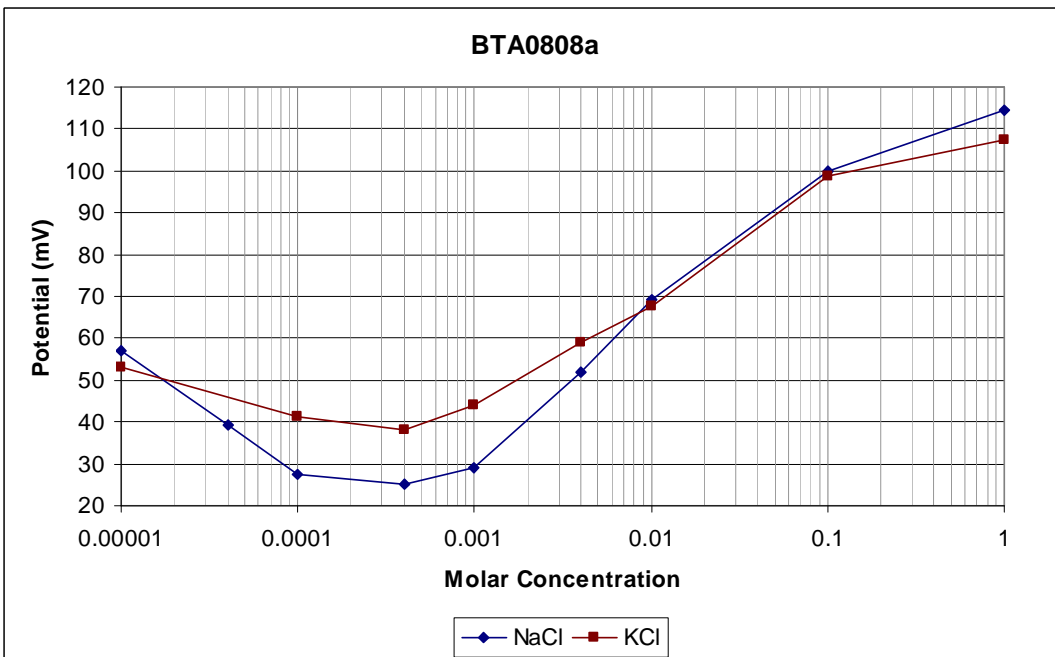
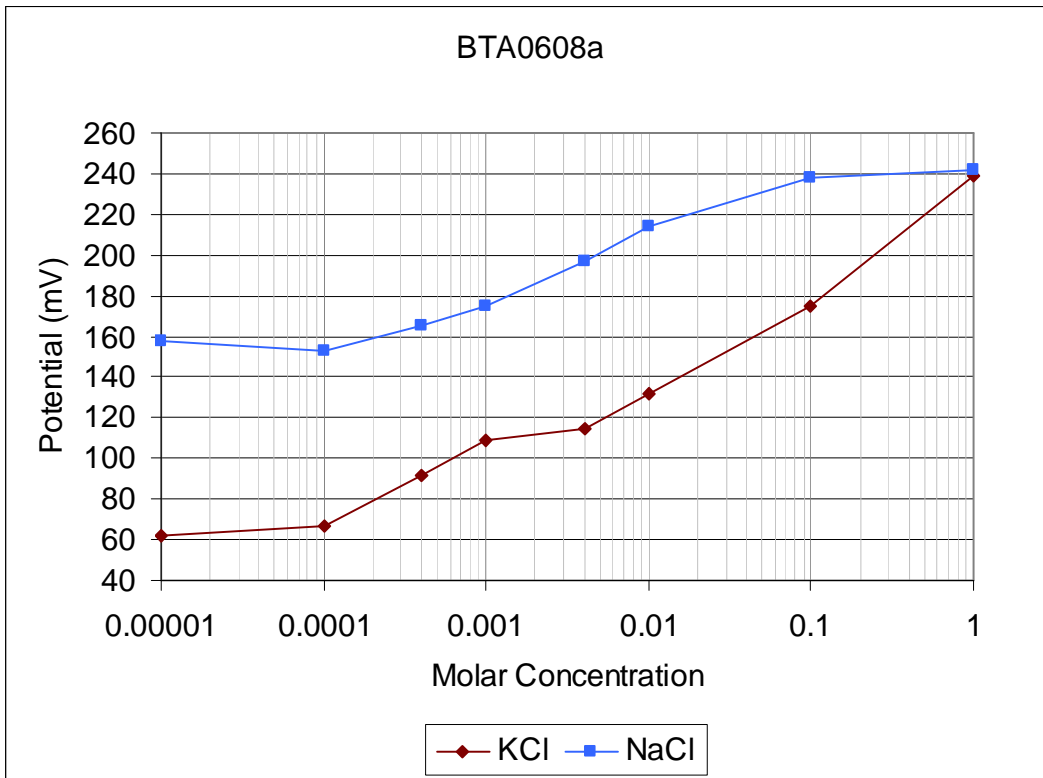
### B1.3 Voltammogram showing the co-polymerization of the BTA ionophore

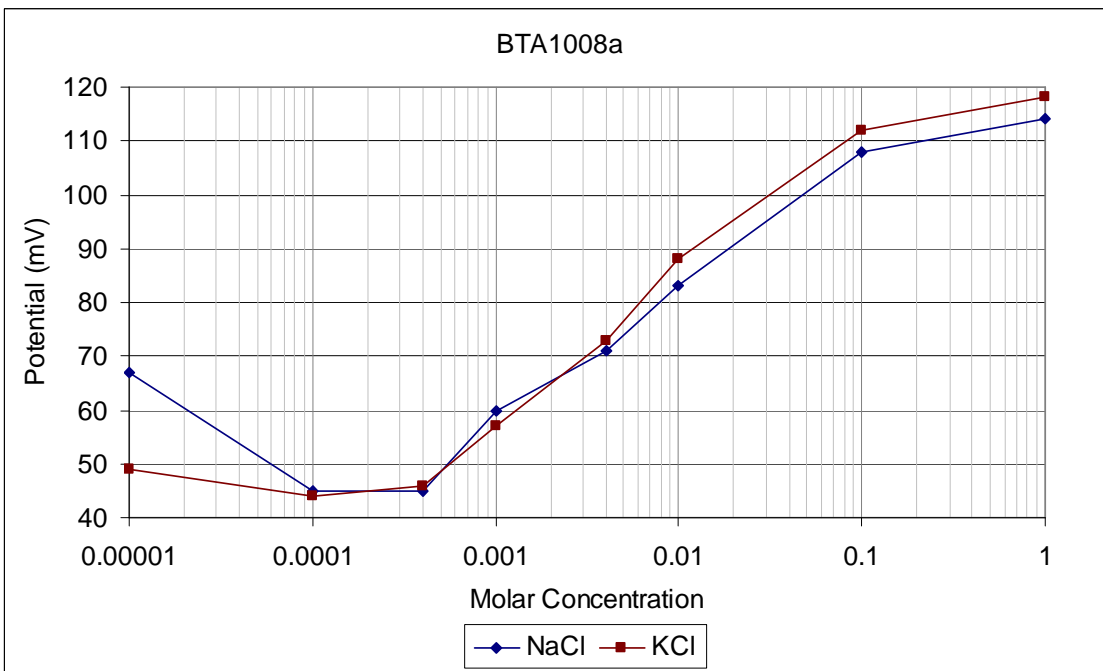
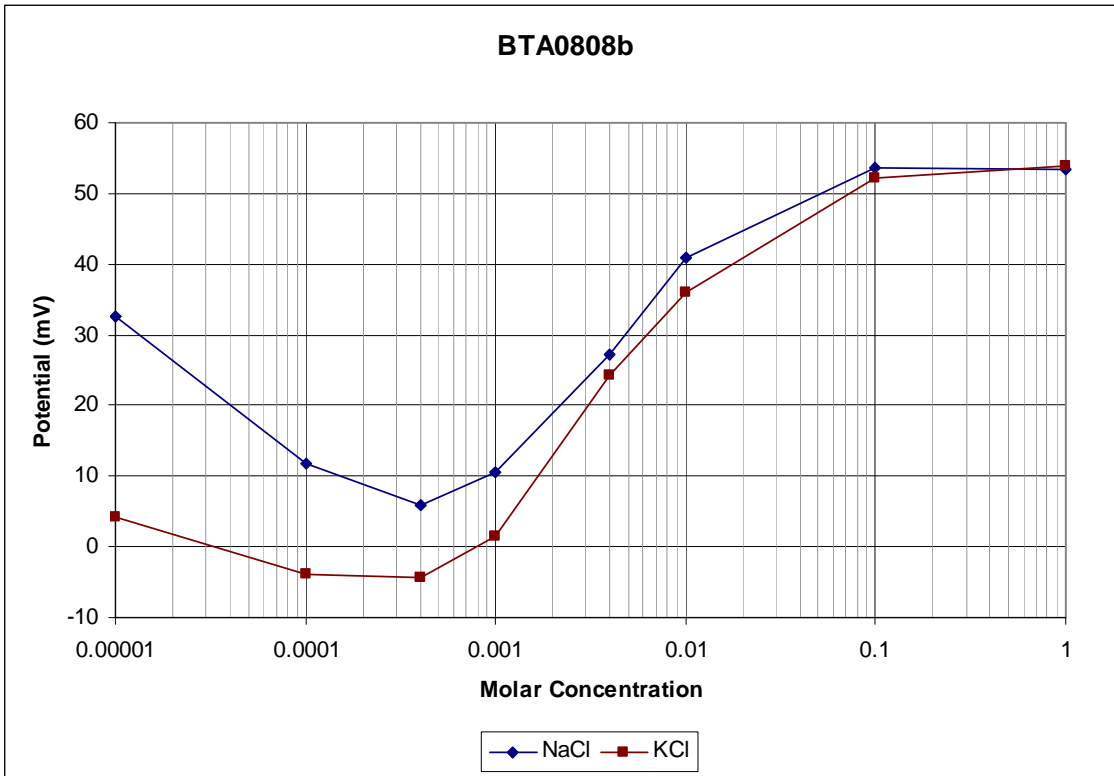


The voltammogram (current in mA vs. potential in mV) of the cyclic voltammetry used to co-polymerize thiophene and the BTA, where the potential (x-axis) was increased at a rate of 10mV/sec from 0-2600mV and then back again. The seven cycles are in order red, blue, green, dark blue, light blue, maroon then black. The measured current (y-axis) is always seen to be higher as the potential increases, and then lower as the potential is decreased back to 0mV. The first peak at approximately 1500-1600mV represents the polymerization of thiophene to thiophene, where as the last peak, at 2600mV represents the polymerization of the thiophene to the BTA. The polymerization process as the potential increases represents the reduction of thiophene and the ionophore forming the thiophene-BTA co-polymer. However, lack of corresponding negative peaks in current on the return cycle show that the polymers were not oxidized again on the return run, and thus that the co-polymerization process is irreversible – thiophene and BTA remain attached to each other. During this process, the sulphur ions in the thiophene become bound to the gold electrode surface, thus producing a solid-state ion selective electrode.

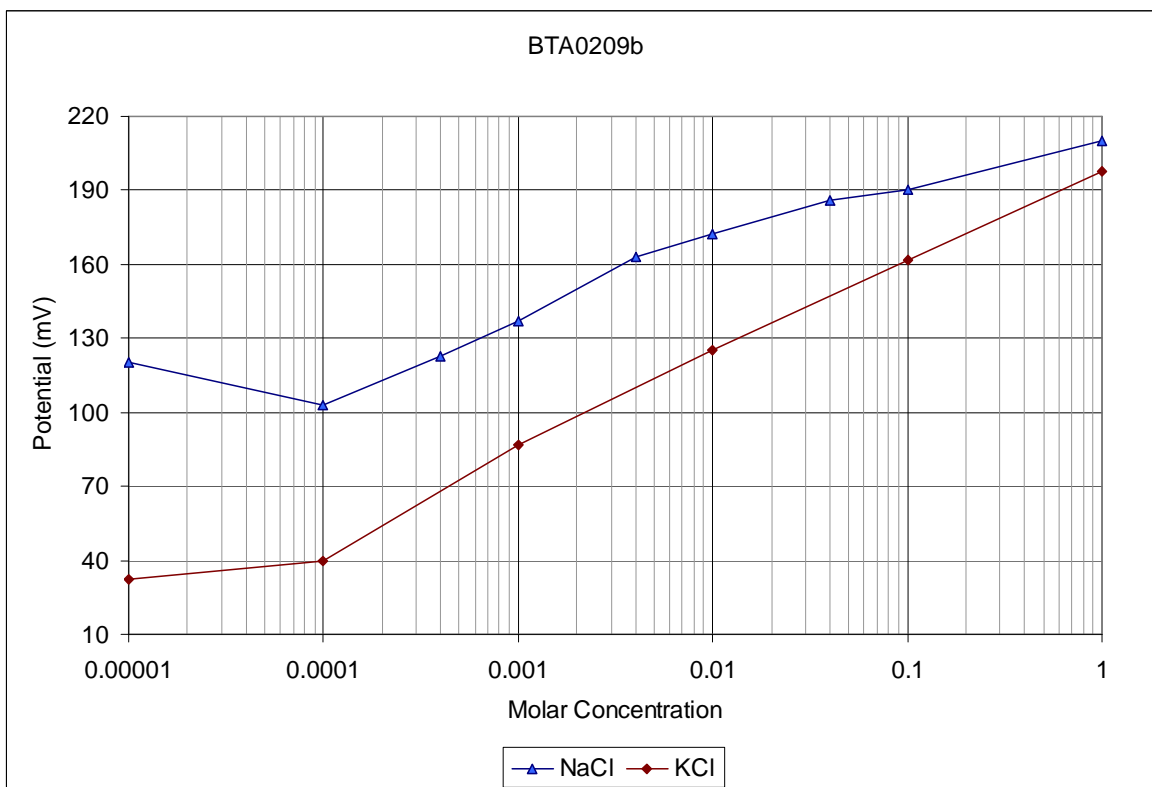
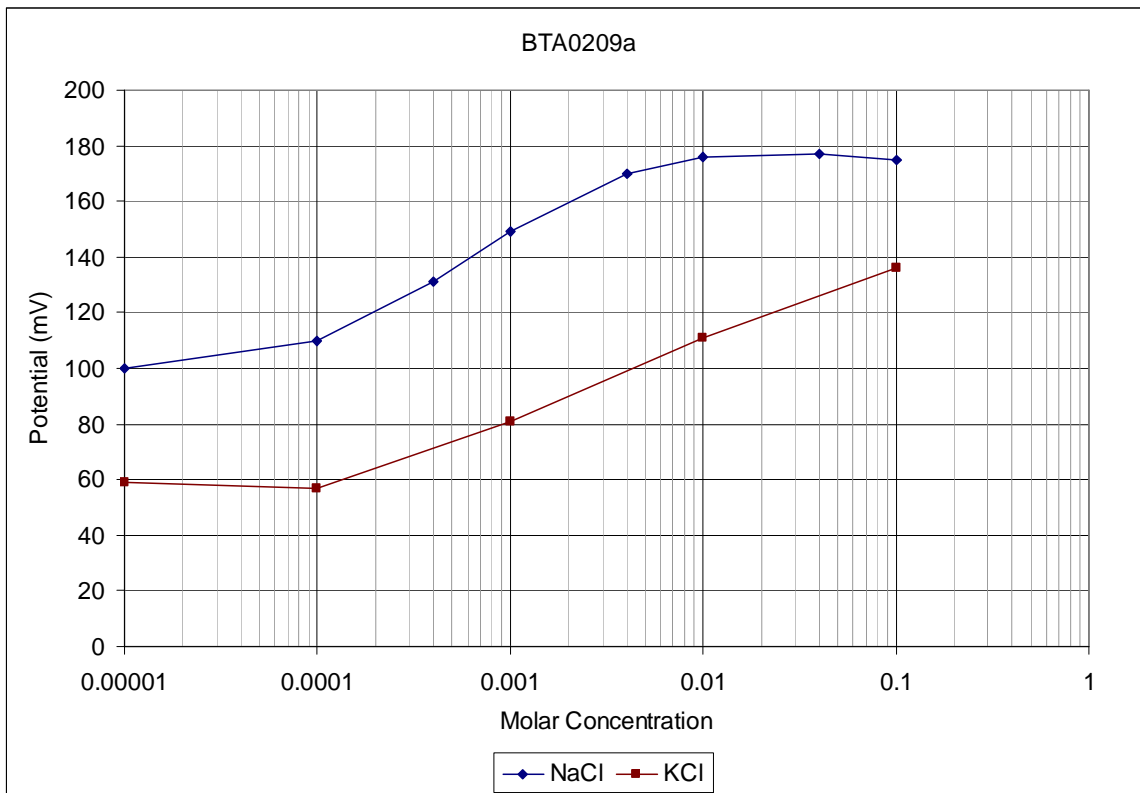
B1.4 Sensor Calibration data for the BTA sensor series, as provided in Table 1, Chapter 4.

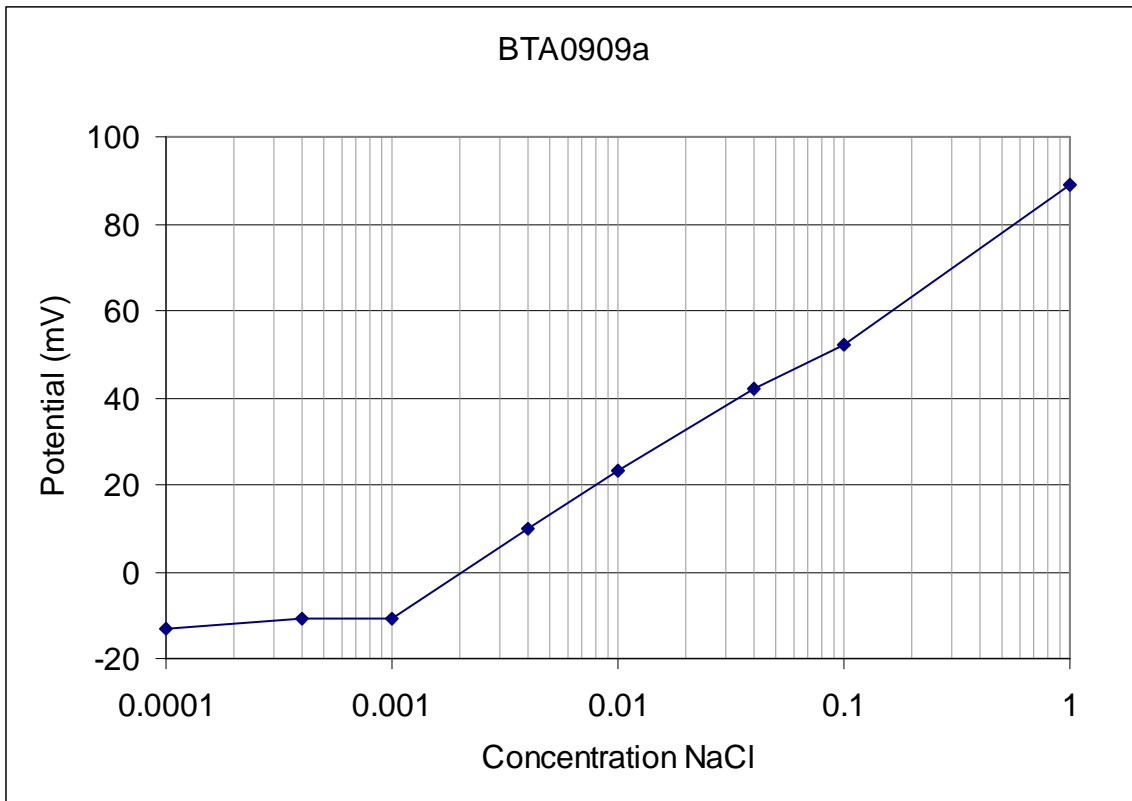




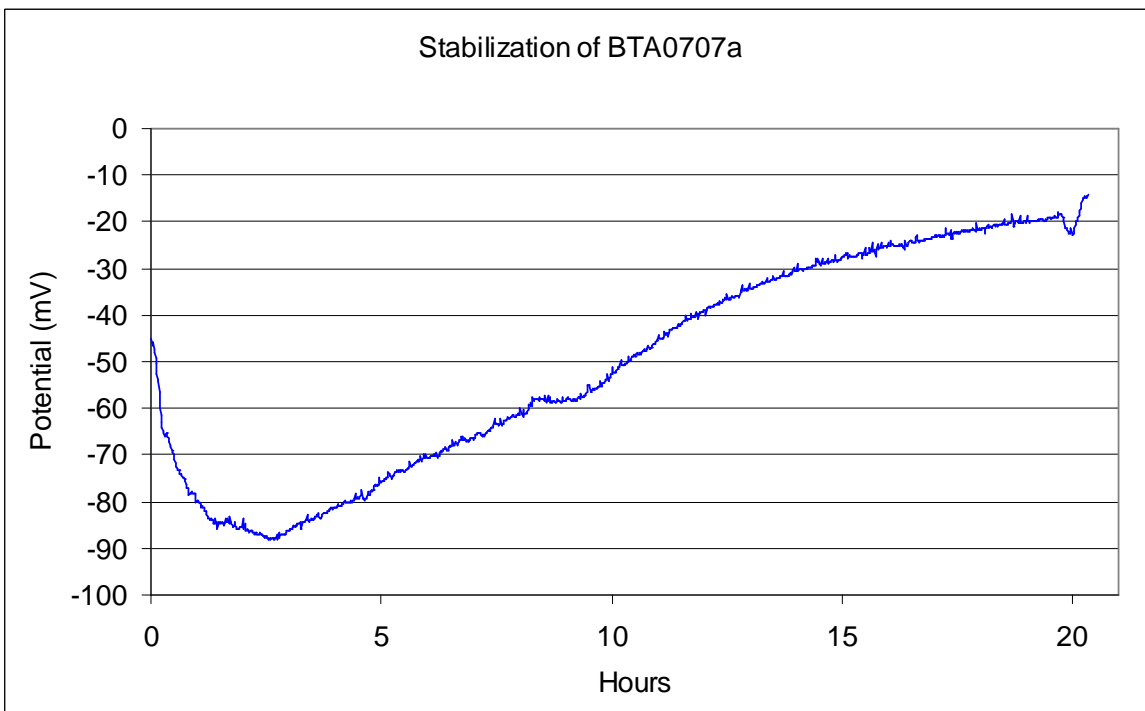




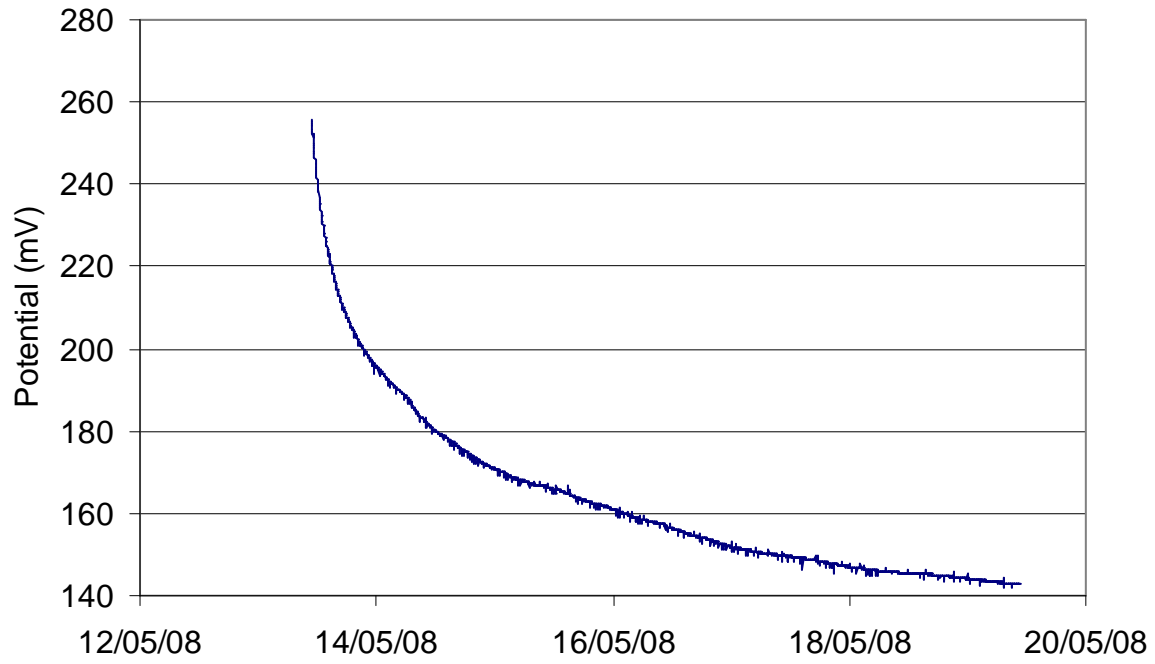




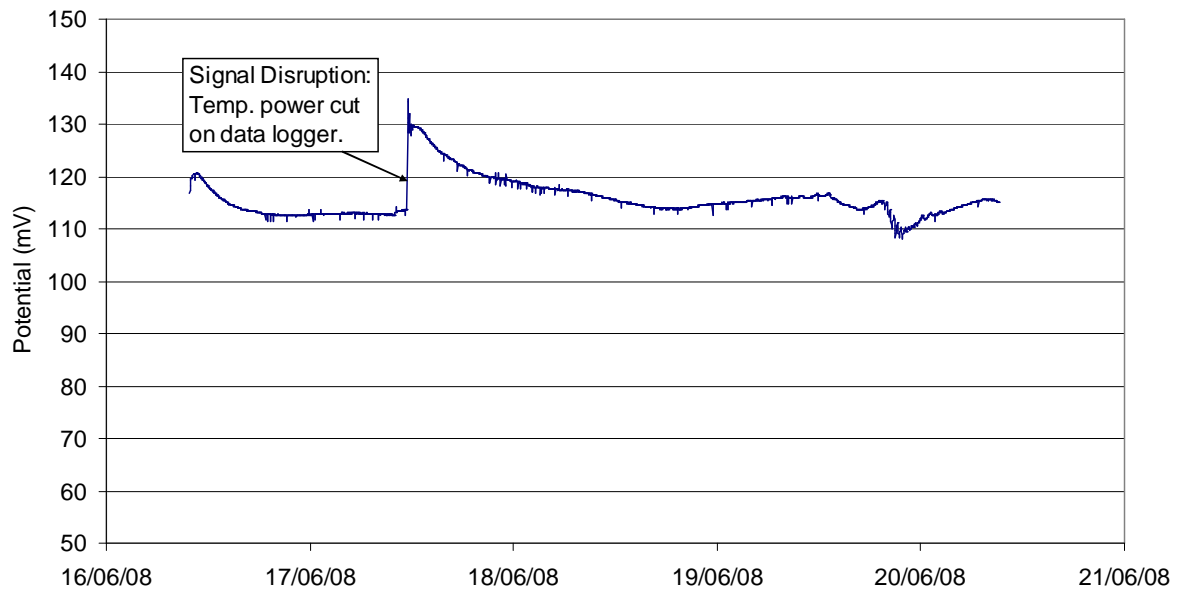
B1.5 Stabilization data for the BTA sensors where long-term testing was conducted.



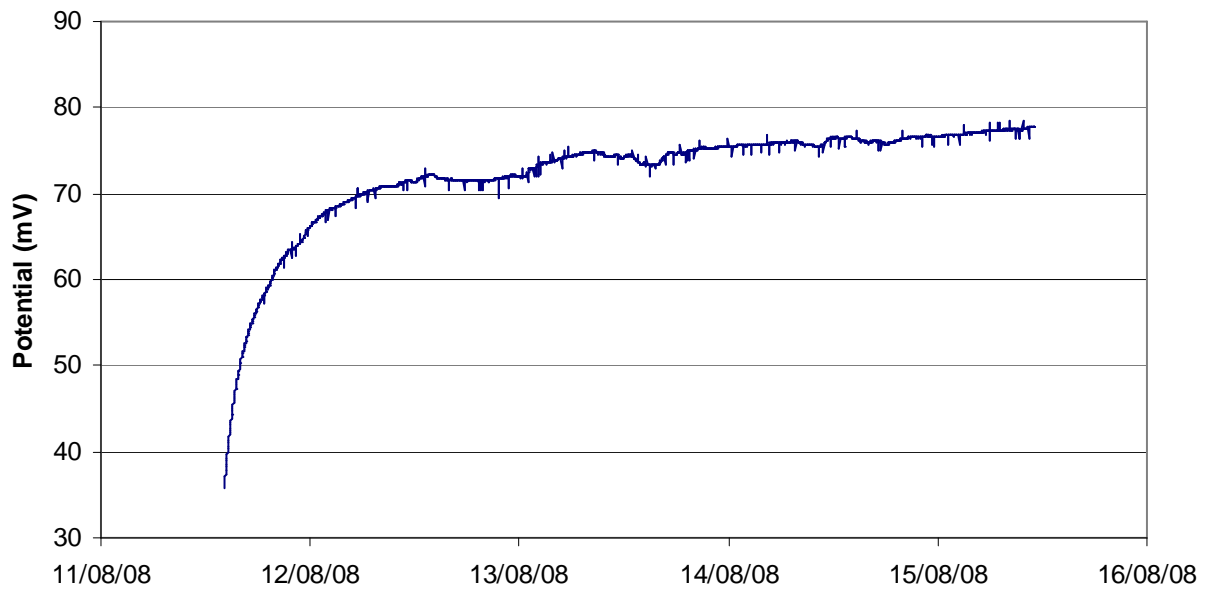
Stabilisation and Drift for BTA0408b



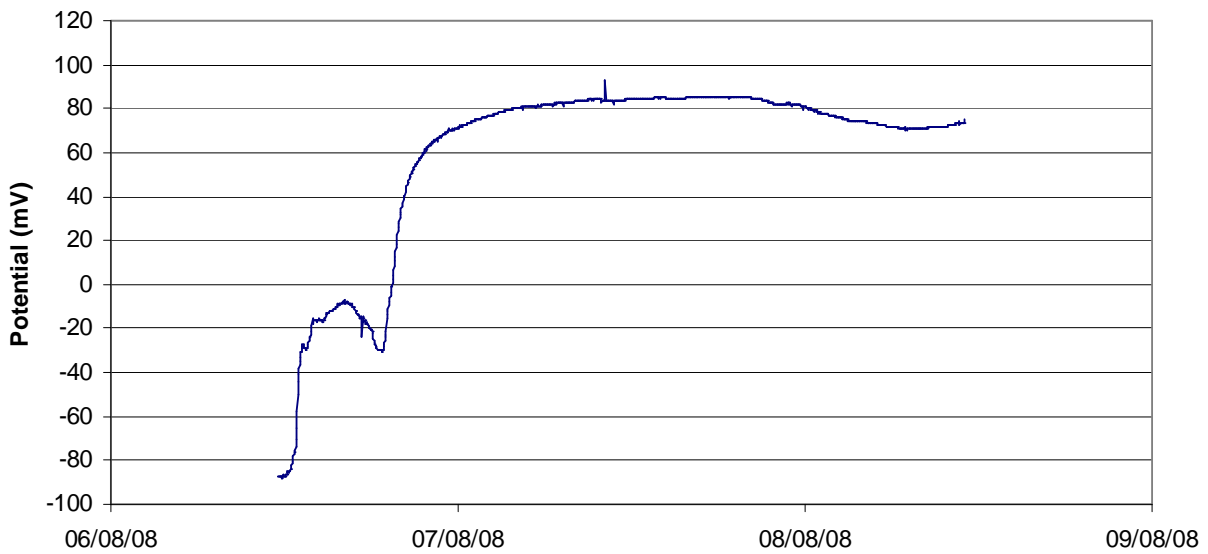
BTA0608 Stability Test



**Stabilization and Drift for BTA0808a**

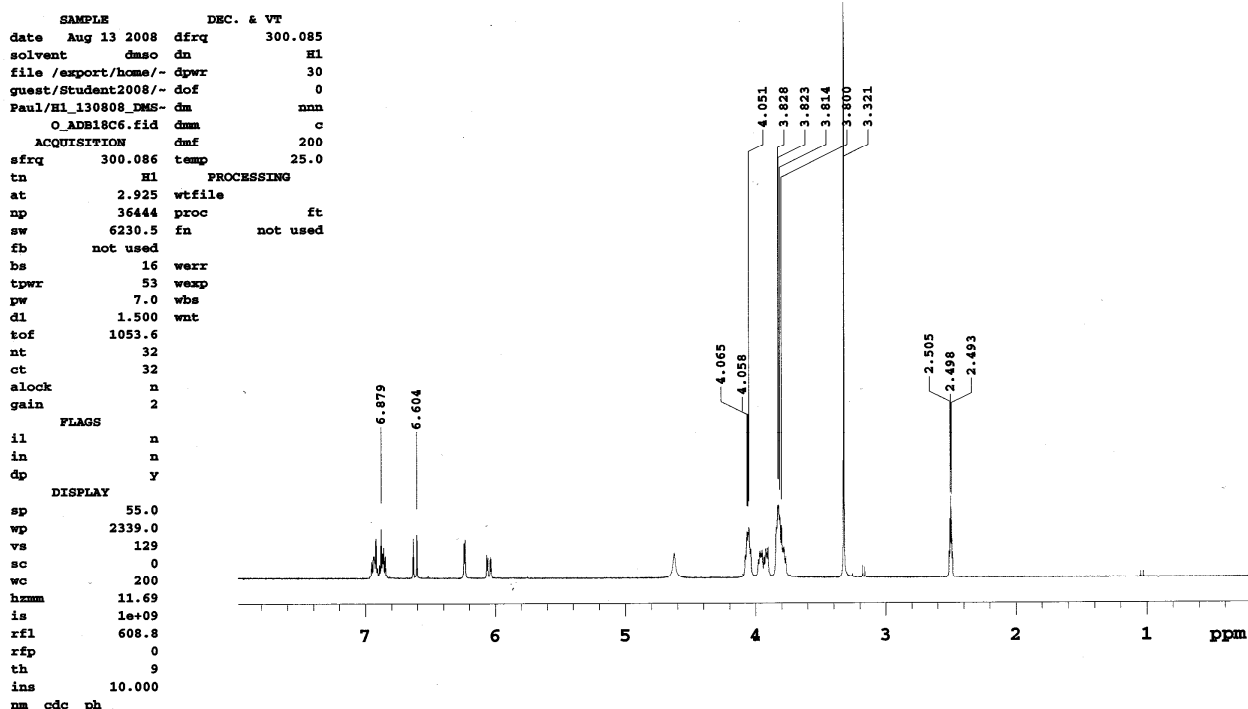


**Stabilization of BTA0808b**

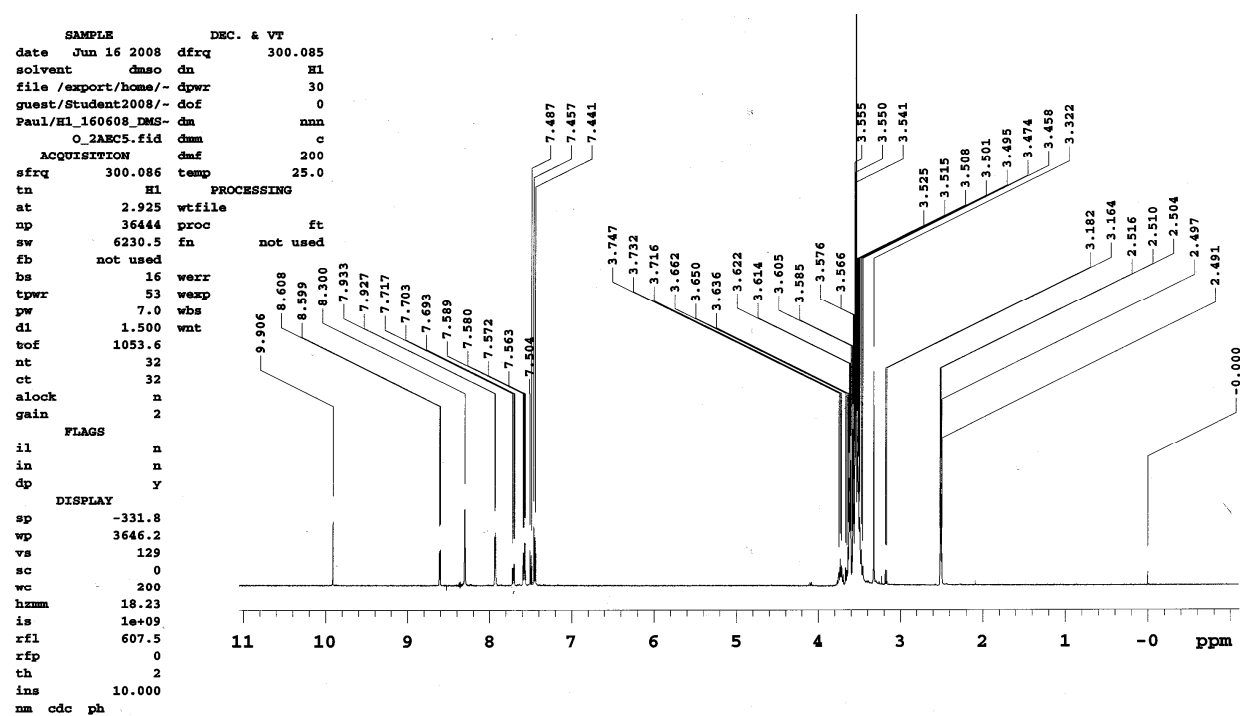


## B2. MTA Sensor Series

### B2.1 NMR Data for the MTA sensors.

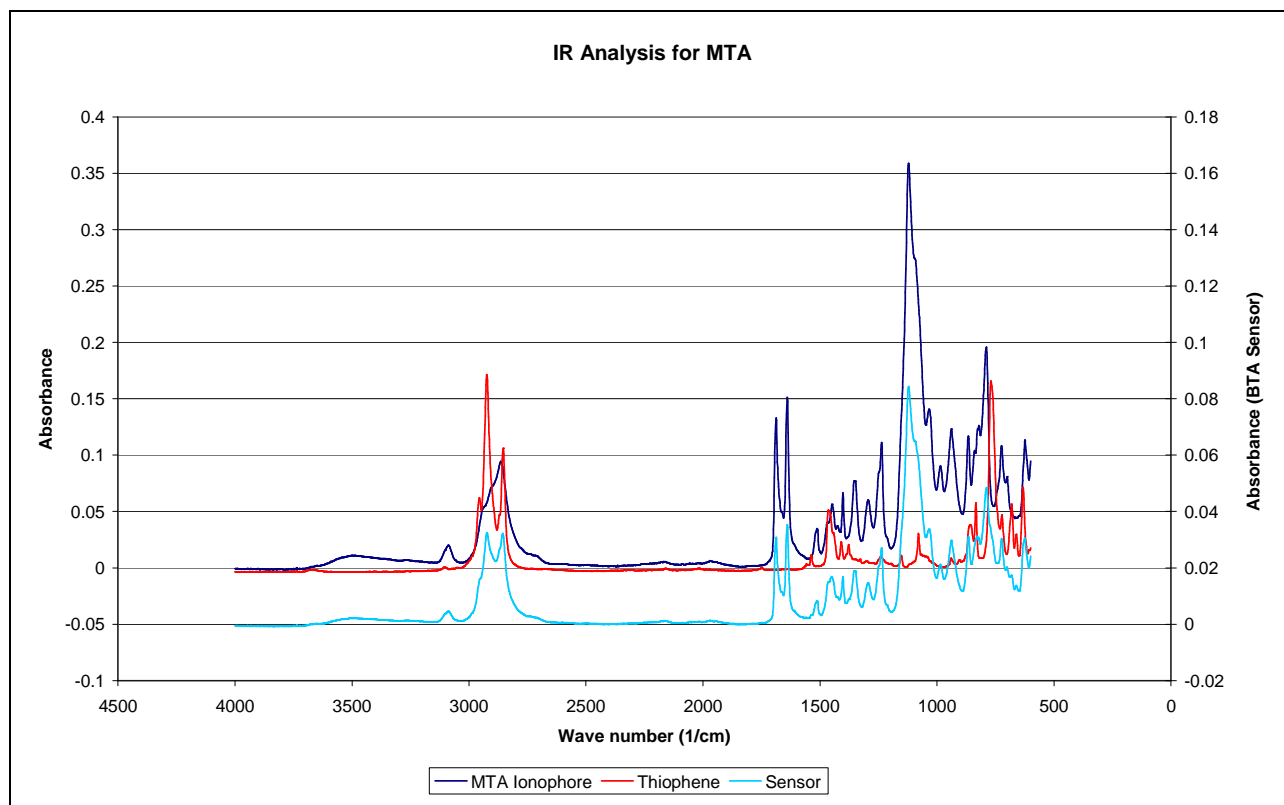


*NMR spectra for the original reagent, 2-aminomethyl-15-crown-5, before the cobbling of the thiophene group to the ionophore.*



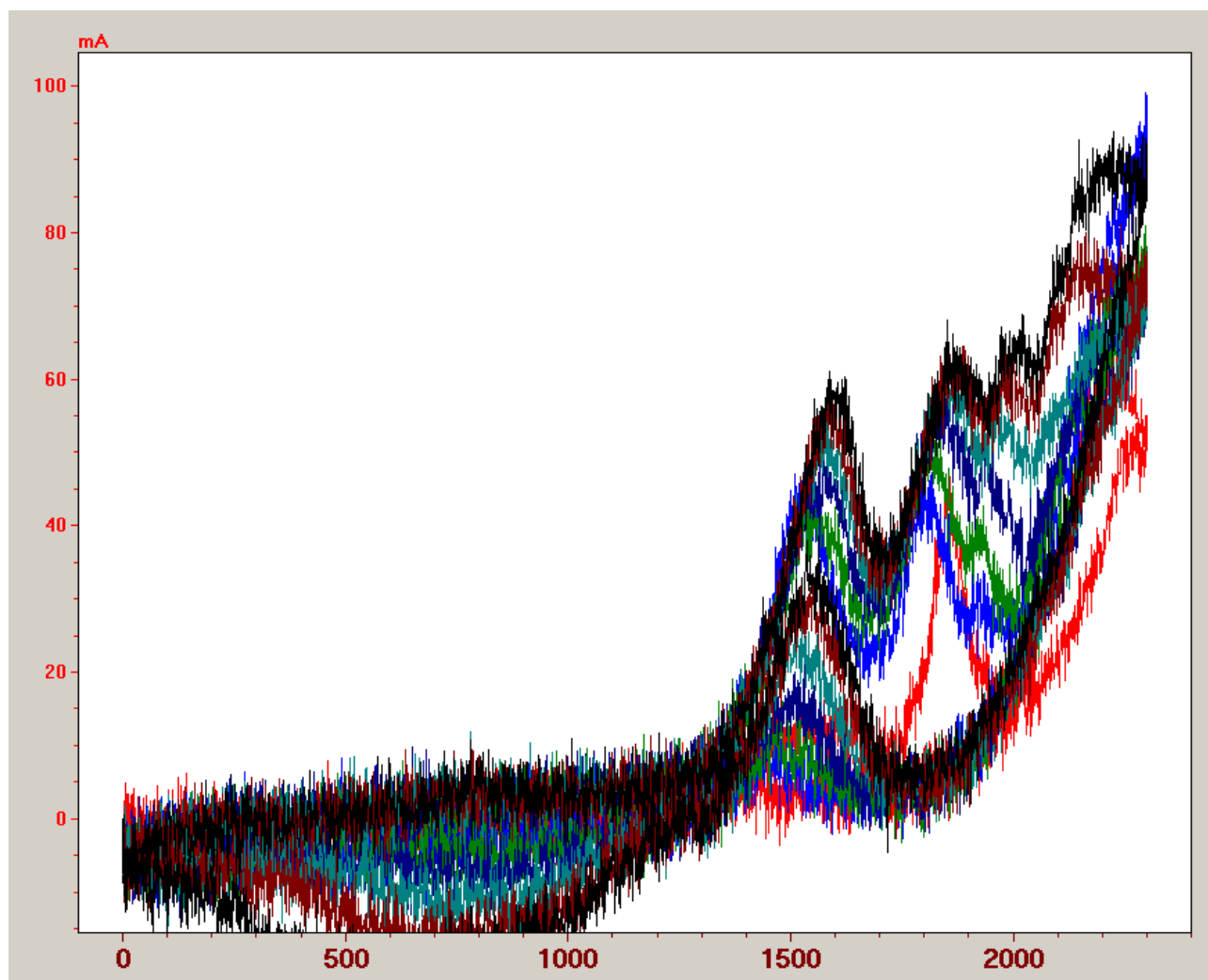
*NMR spectra for the MTA ionophore. Note the hydrogen peaks from between 6 and 7ppm in the reagent to between 7.5 and 8.5 in the MTA (product) indicating that the reaction went to completion.*

## B2.2 Infrared spectra for the MTA sensors



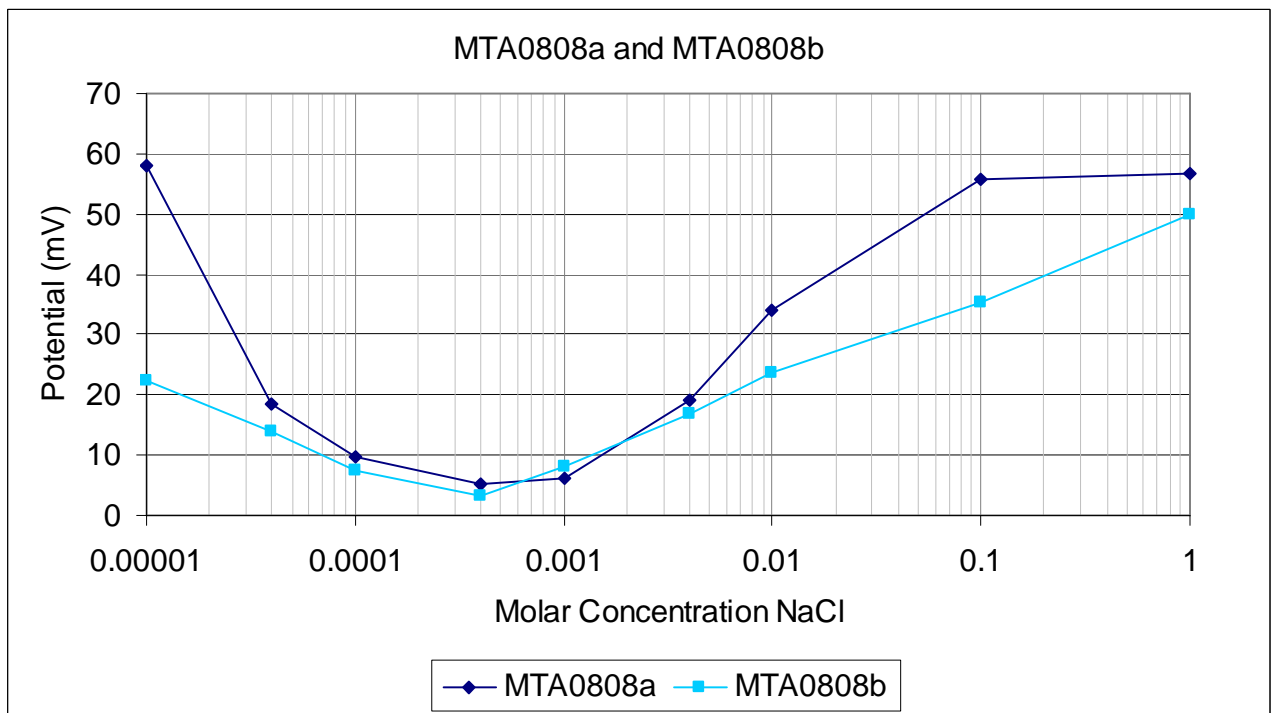
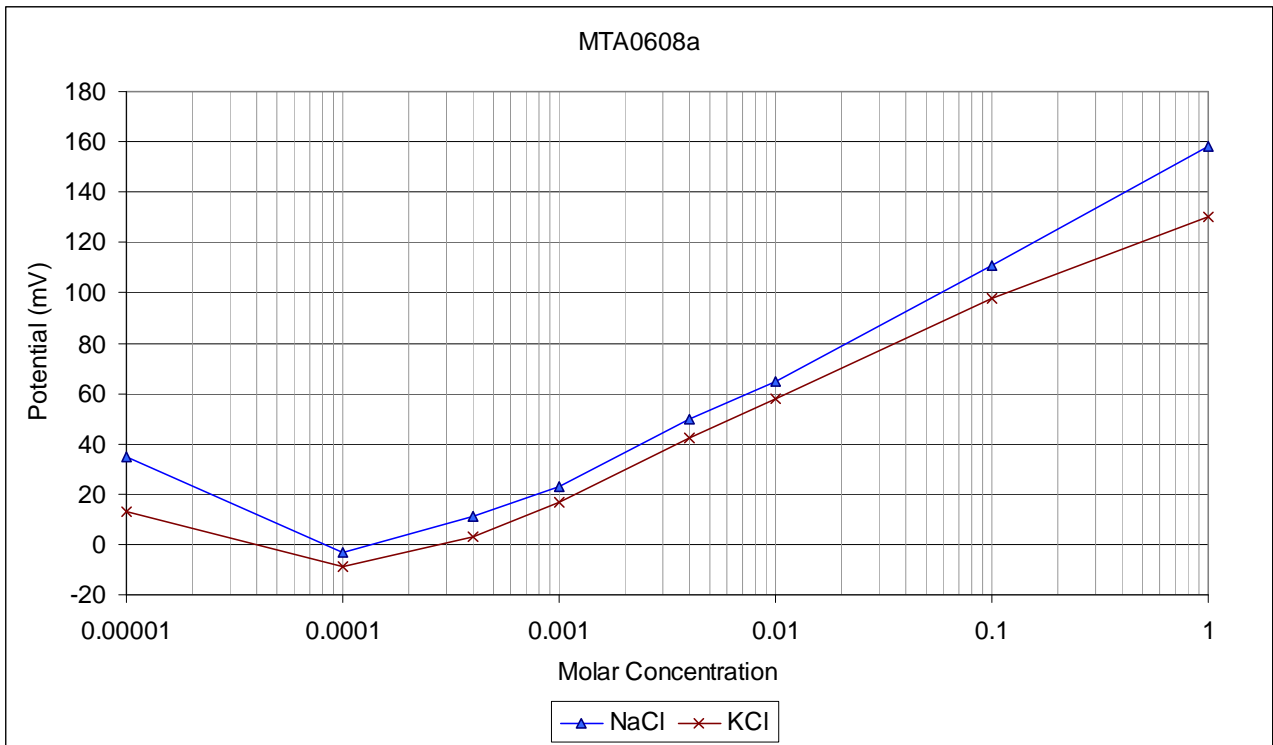
*Infrared absorbance data for the MTA sensor (light blue), where the ionophore and thiophene has been co-polymerized on the gold electrode. For reference, there is also infrared absorbance data for the ionophore (dark blue) and thiophene (red) before polymerisation. From the data, it is apparent that the sensor has predominately the signal of the MTA ionophore, indicating that the ionophore was successfully attached to the gold surface.*

### B2.3 Voltammogram showing the co-polymerization of the MTA ionophore

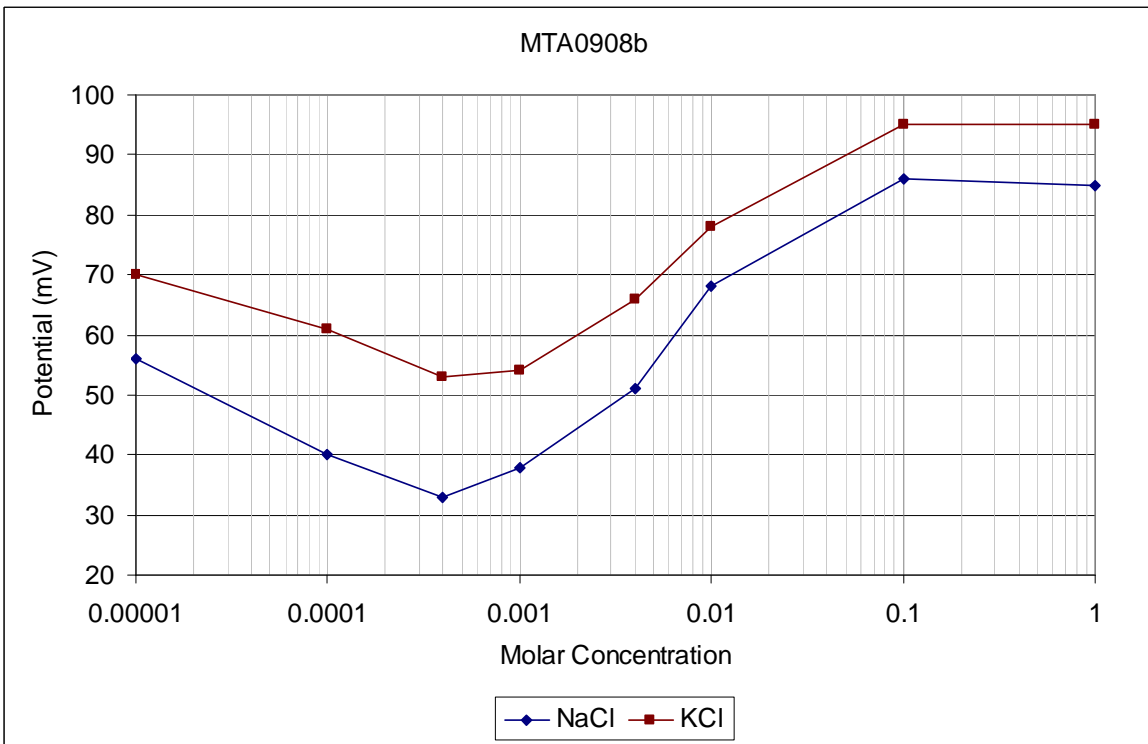
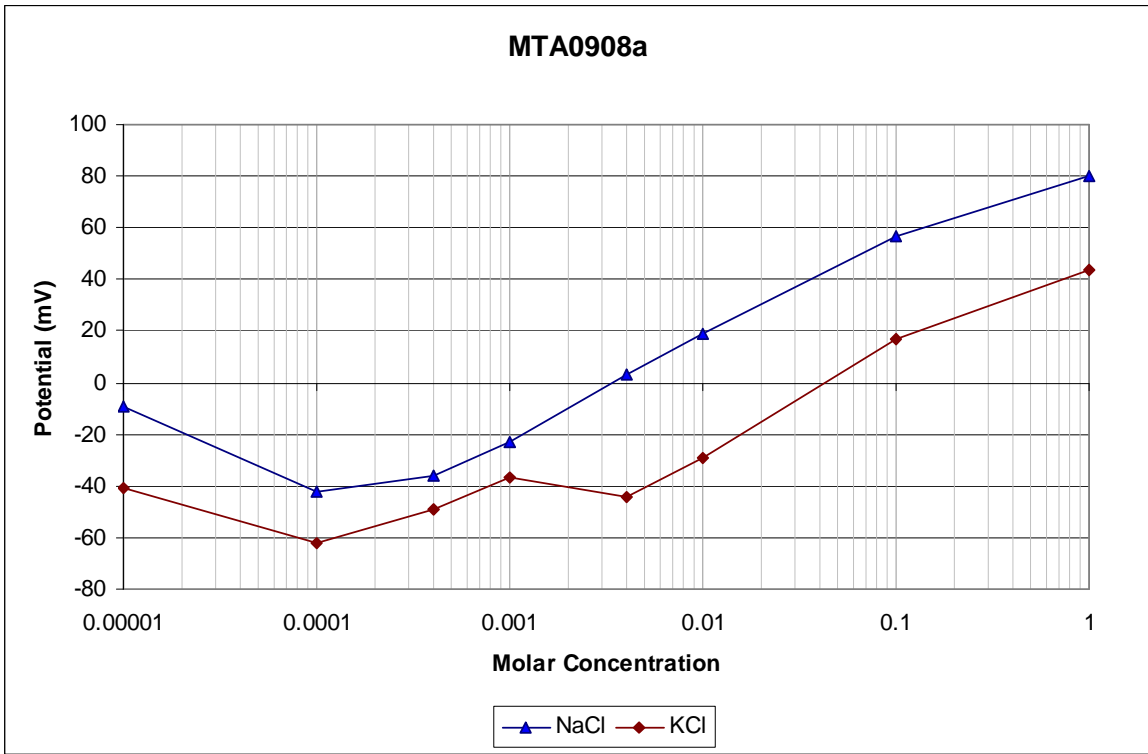


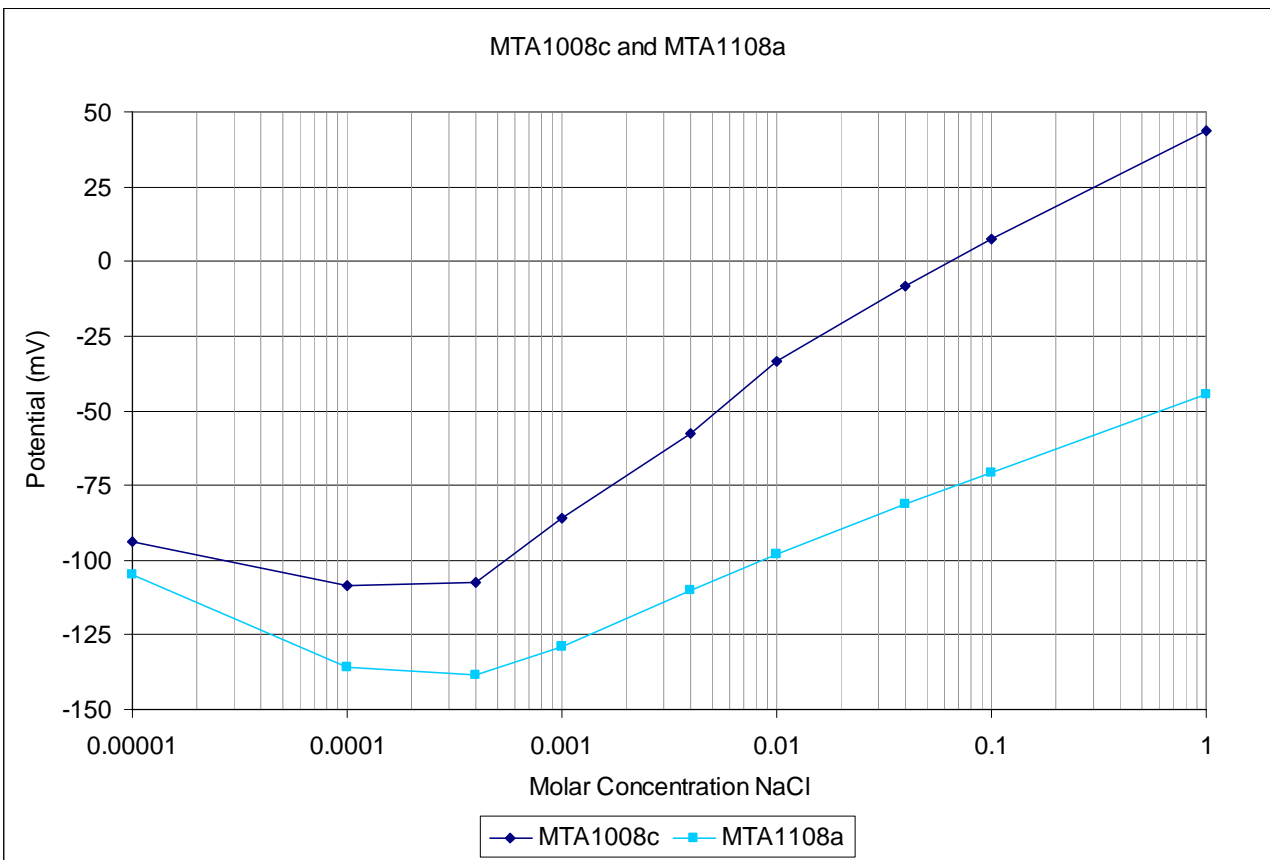
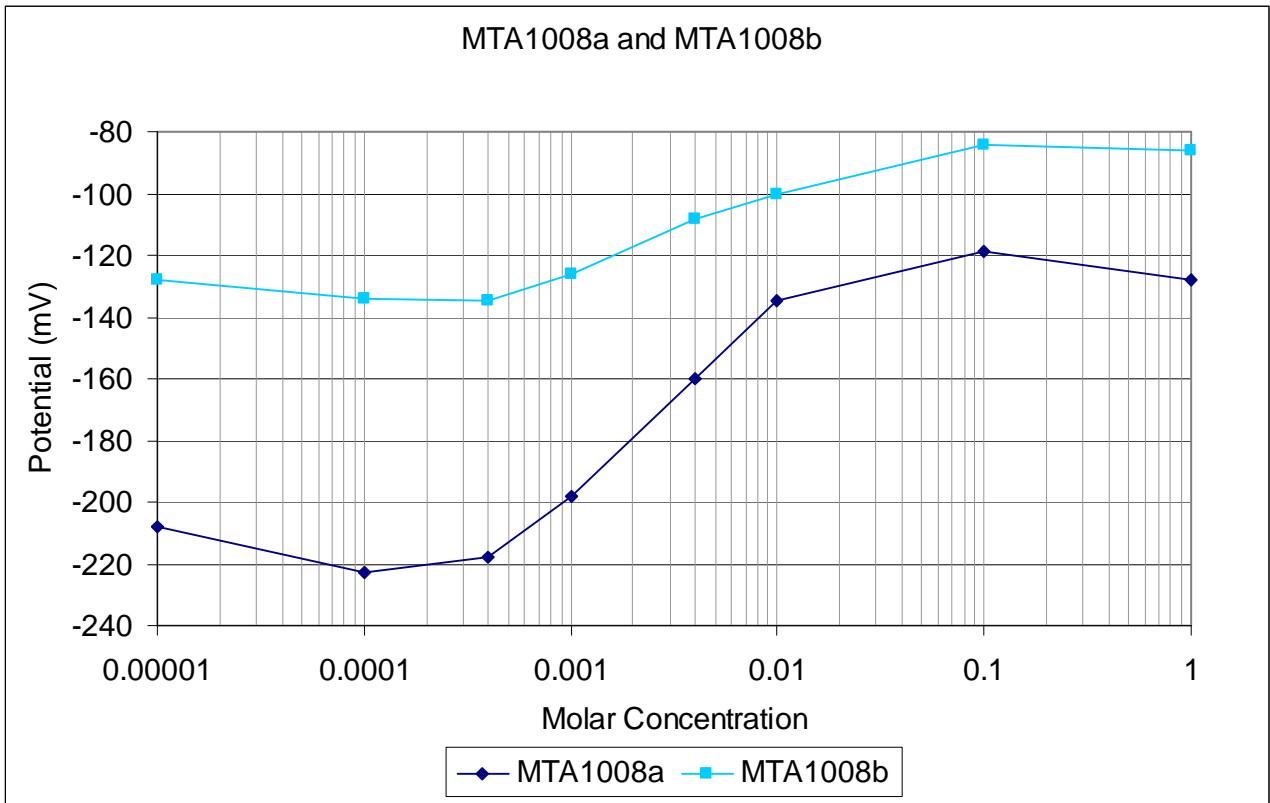
*The voltammogram (current in mA vs. potential in mV) of the cyclic voltammetry used to co-polymerize thiophene and the MTA, where the potential (x-axis) was increased at a rate of 10mV/sec from 0-2400mV and then back again. The seven cycles are in order red, blue, green, dark blue, light blue, maroon then black. The measured current (y-axis) is always seen to be higher as the potential increases, and then lower as the potential is decreased back to 0mV. The first peak at approximately 1500-1600mV represents the polymerization of thiophene to thiophene, where as the last peak, at 2400mV represents the polymerization of the thiophene to the MTA. The polymerization process as the potential increases represents the reduction of thiophene and the ionophore forming the thiophene-MTA co-polymer. However, lack of corresponding negative peaks in current on the return cycle show that the polymers were not oxidized again on the return run, and thus that the co-polymerization process is irreversible – thiophene and MTA remain attached to each other. During this process, the sulphur ions in the thiophene become bound to the gold electrode surface, thus producing a solid-state ion selective electrode.*

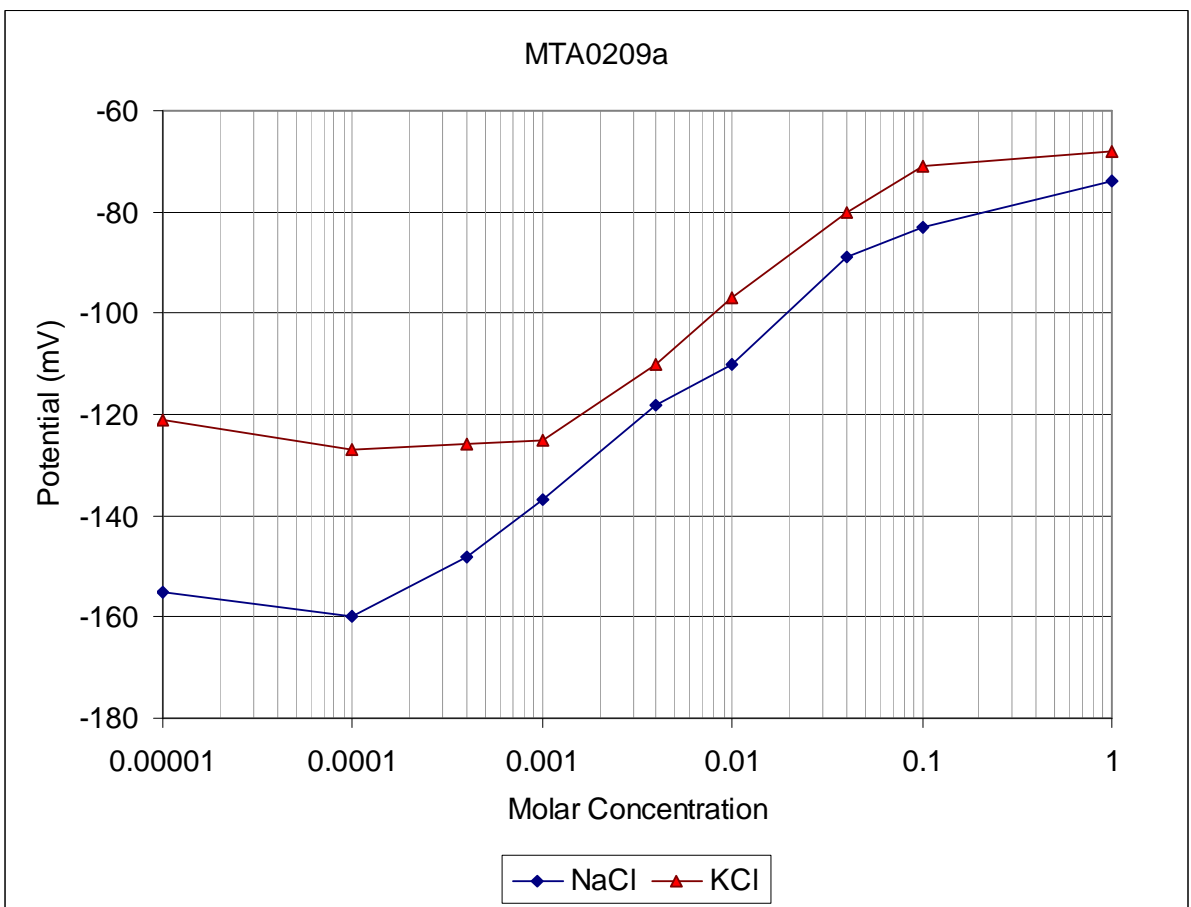
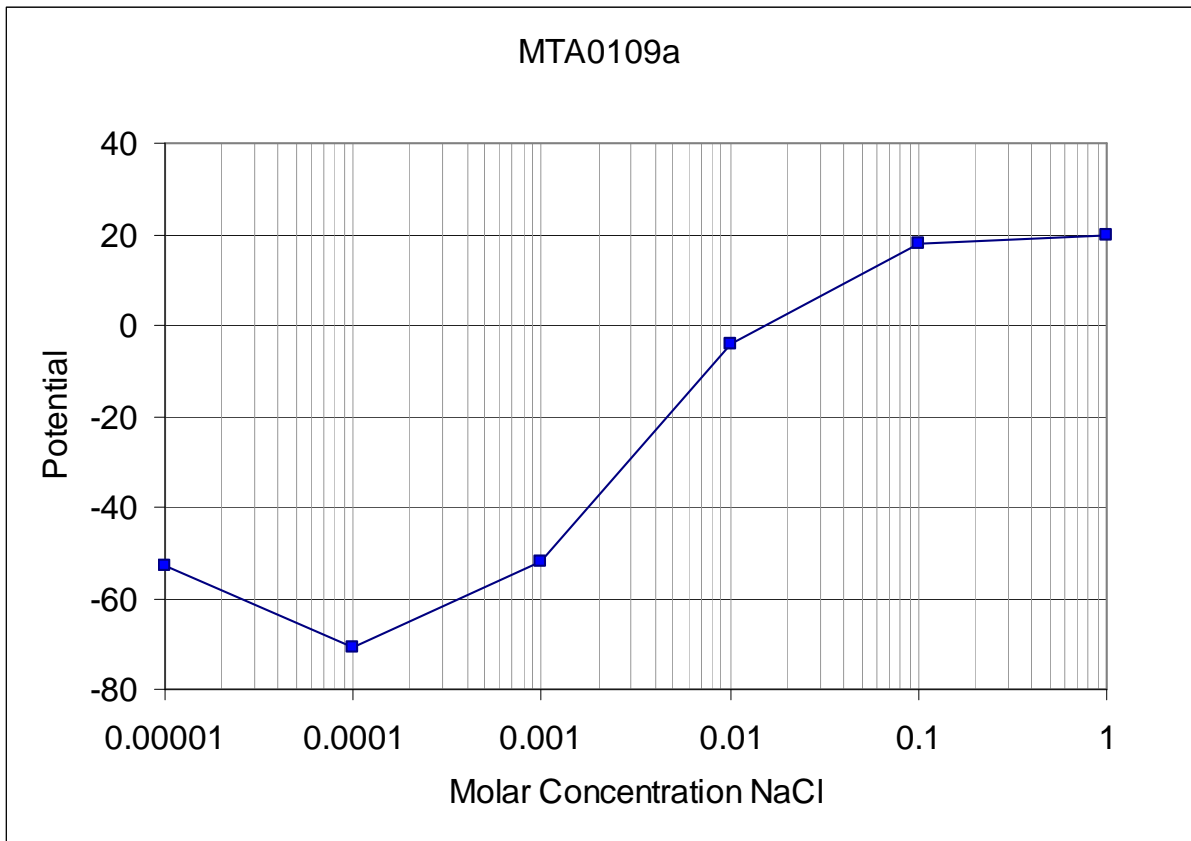
B2.4 Sensor Calibration data for the MTA sensor series, as provided in Table 2, Chapter 4.



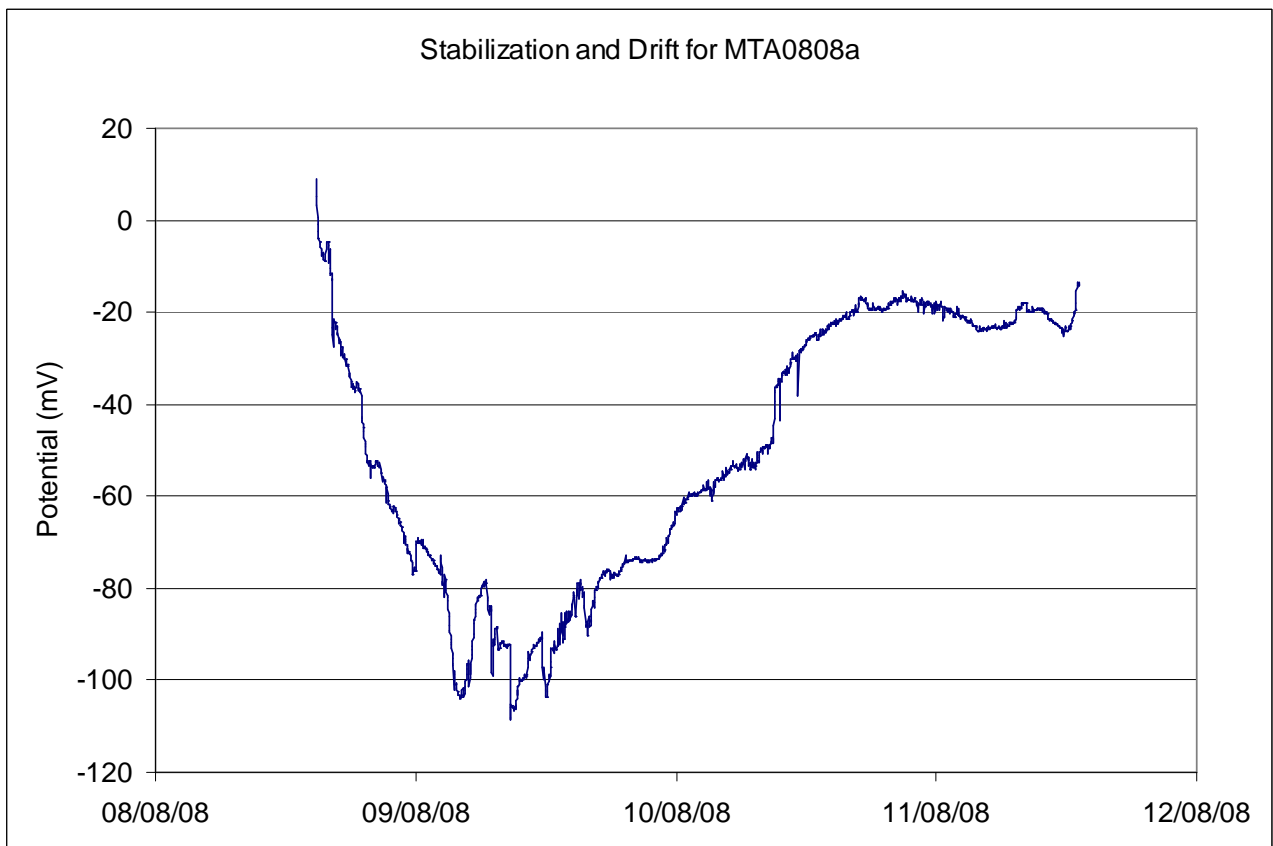
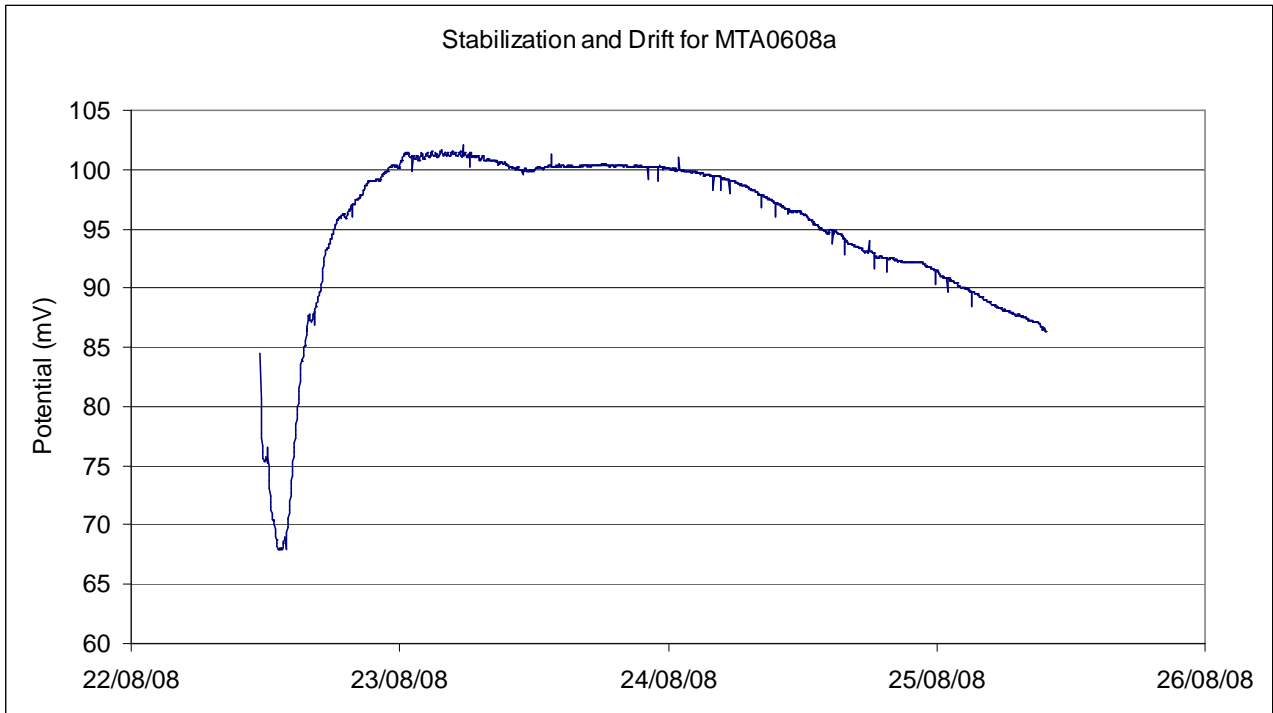


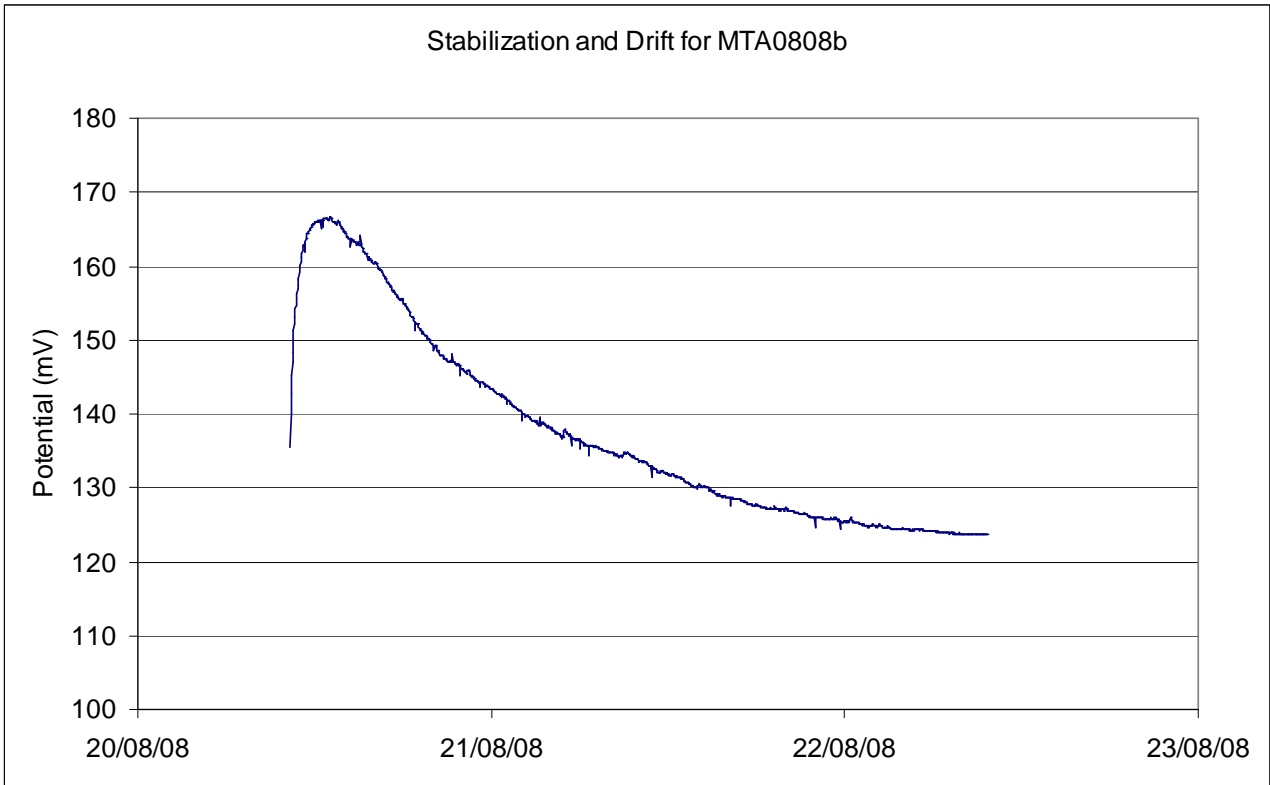






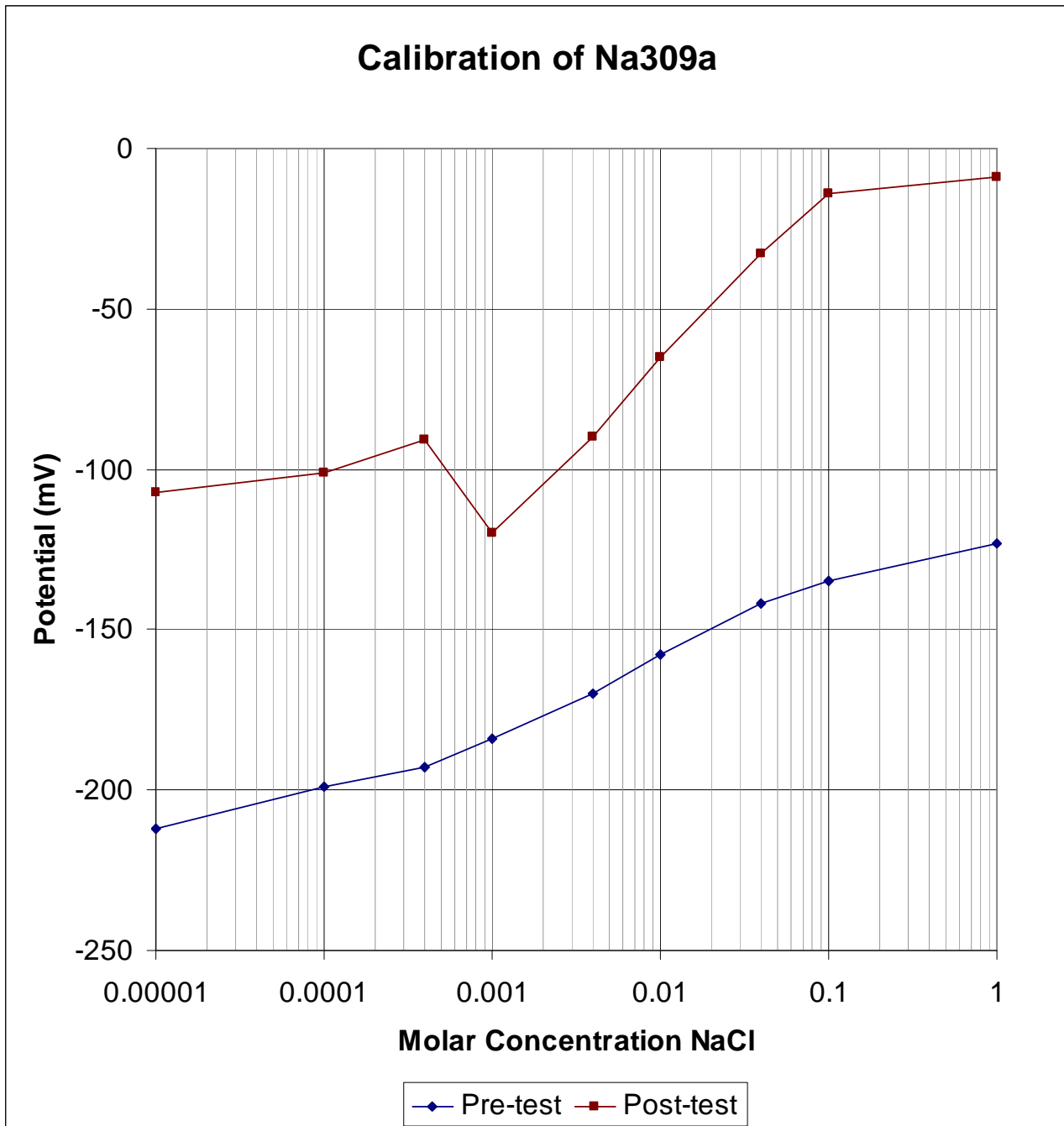
B2.5 Stabilization data for the MTA sensors where long-term testing was conducted.



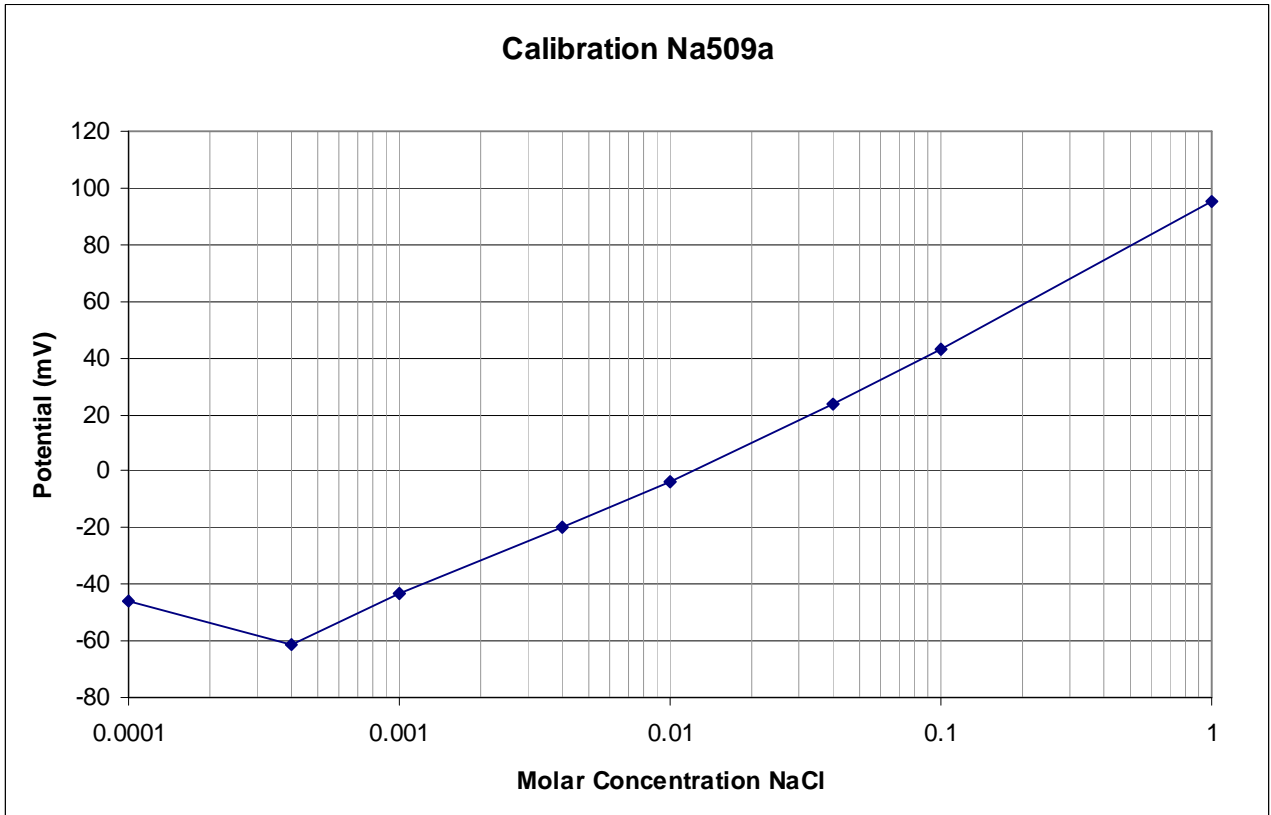
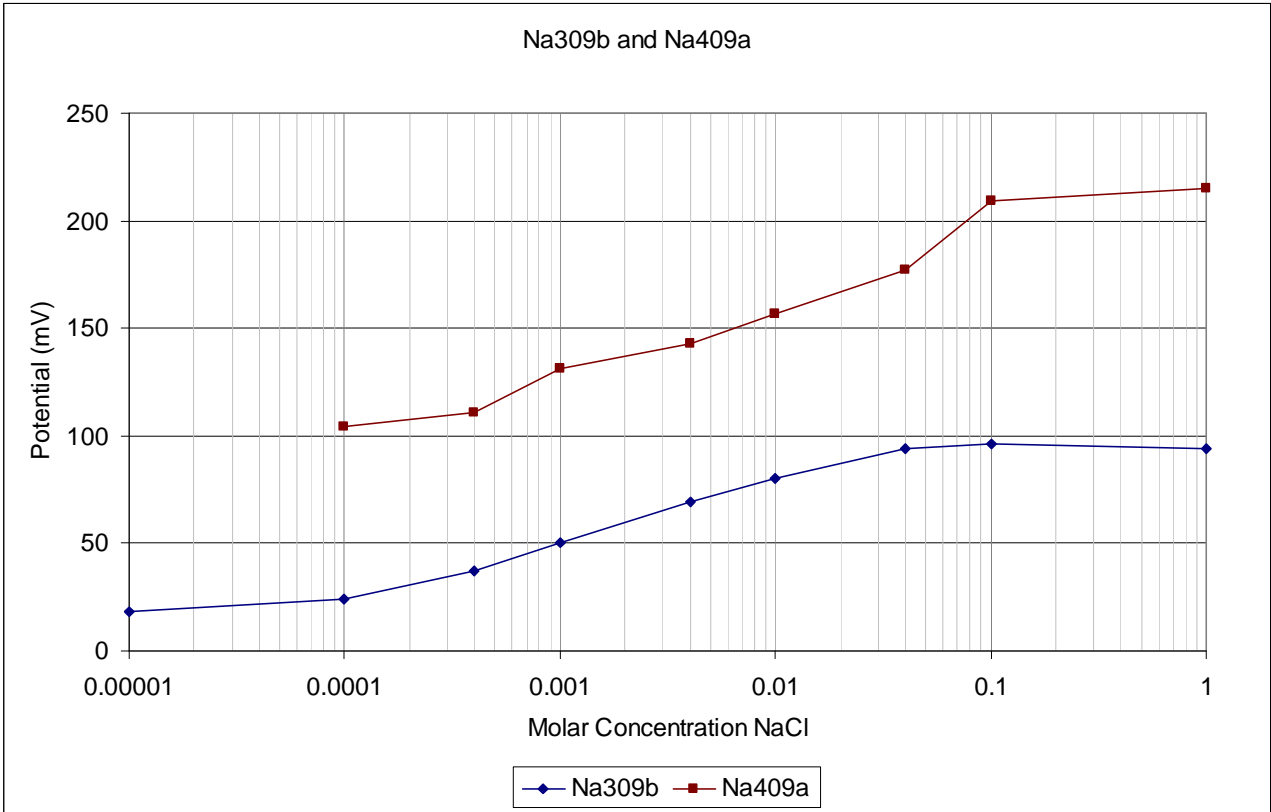


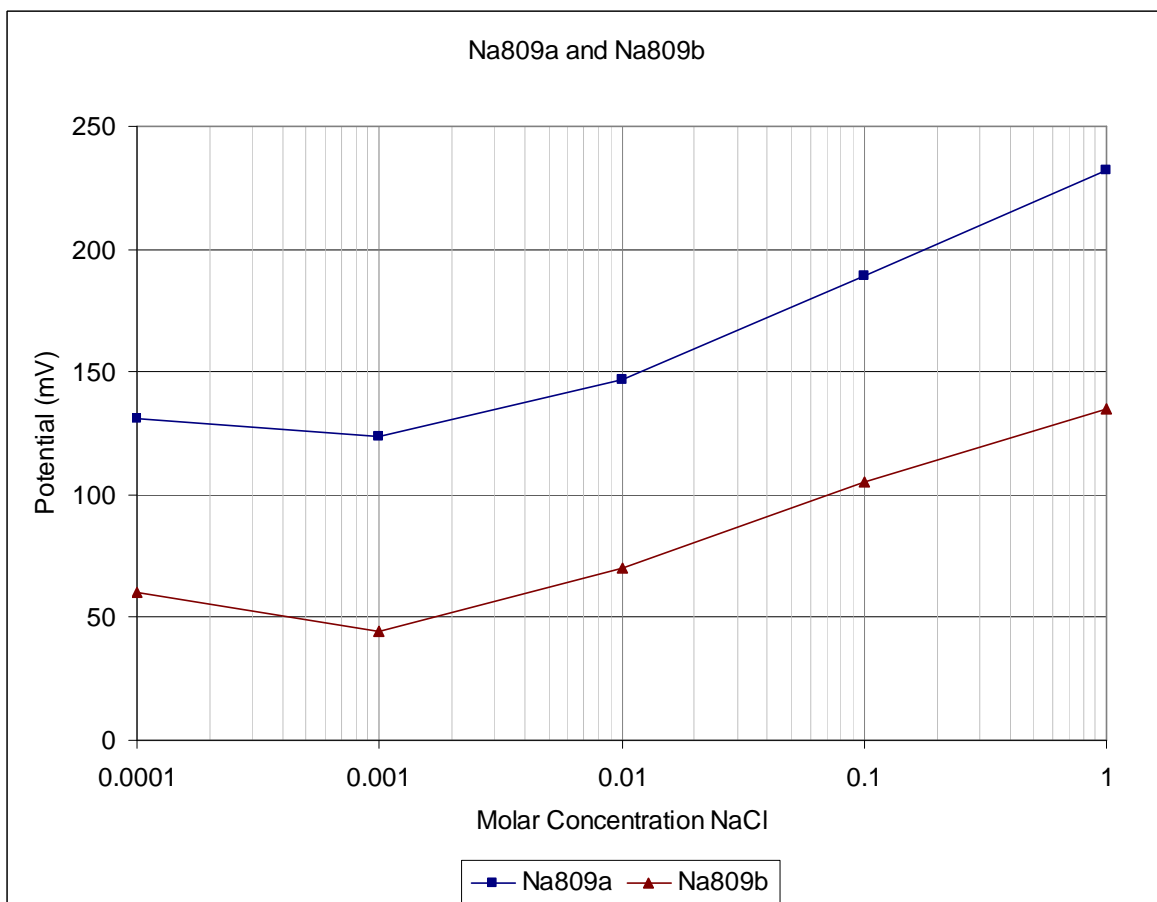
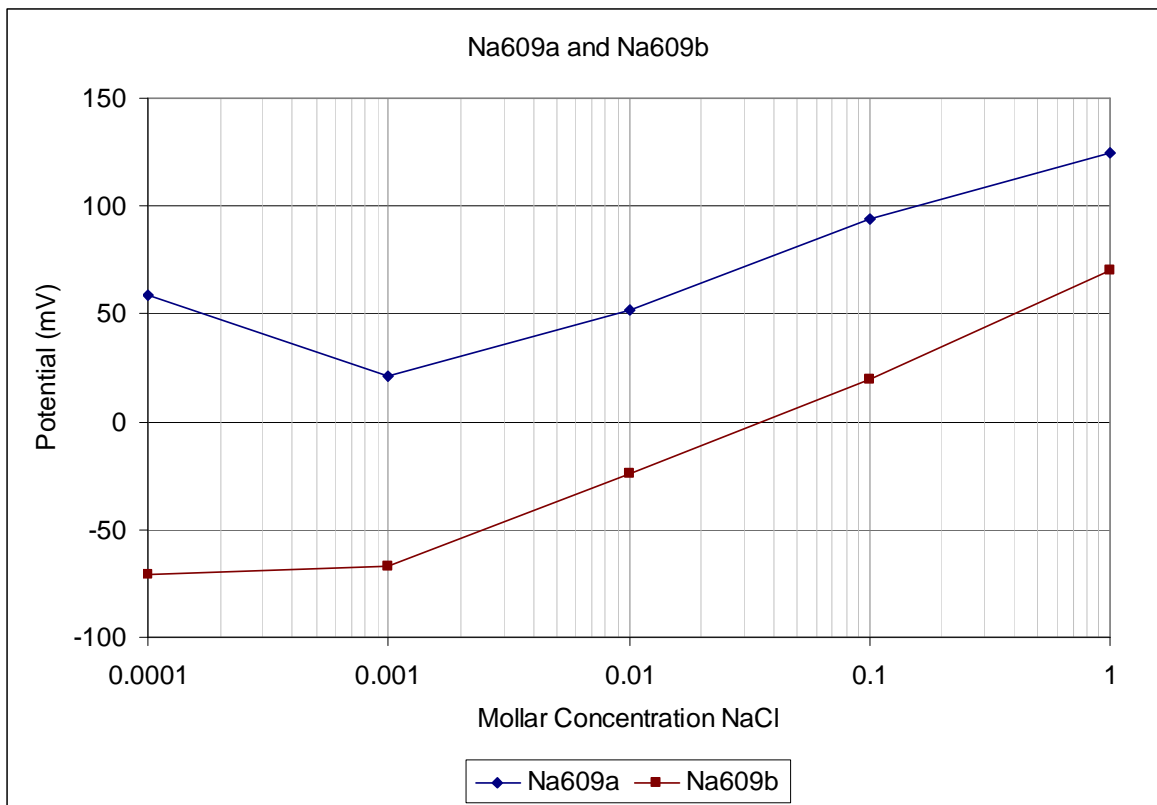
### B3. PVC Sensor Series

B3.1 Sensor Calibration data for the PVC sensor series, as provided in Table 3, Chapter 4.

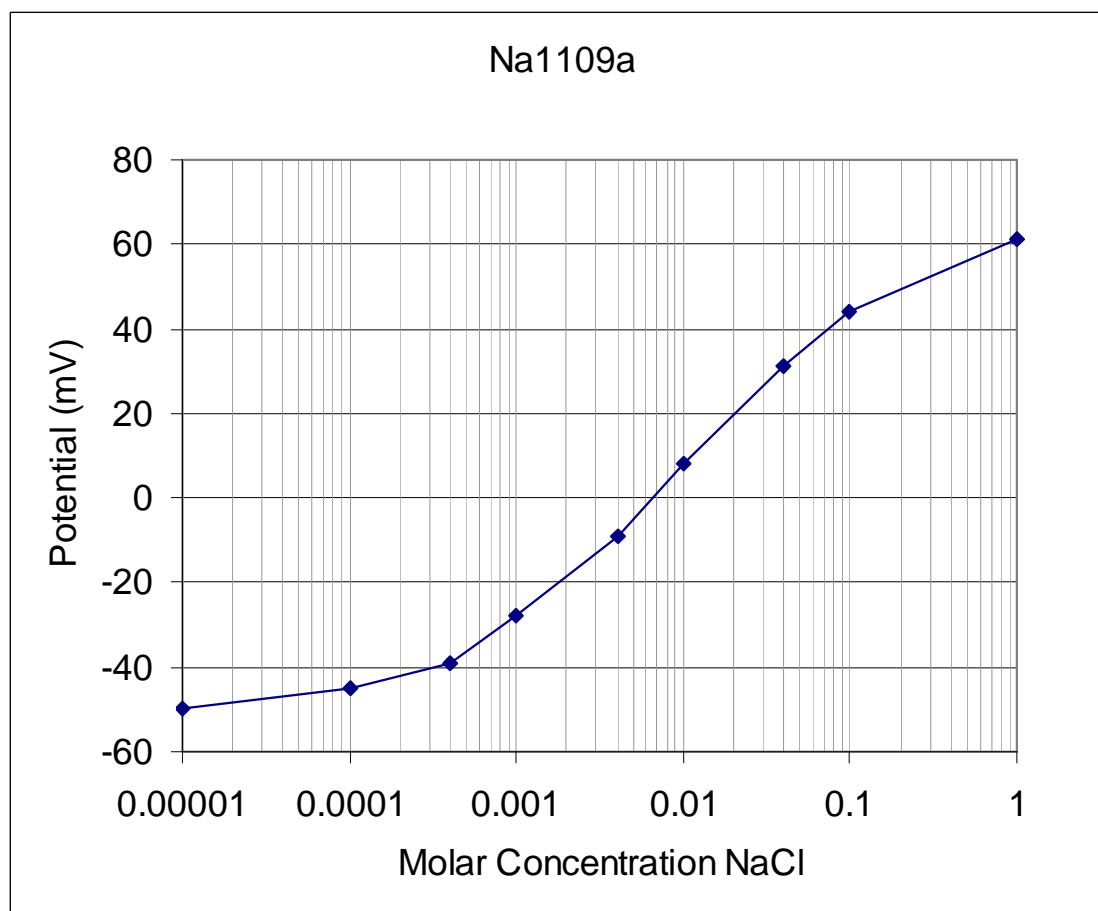
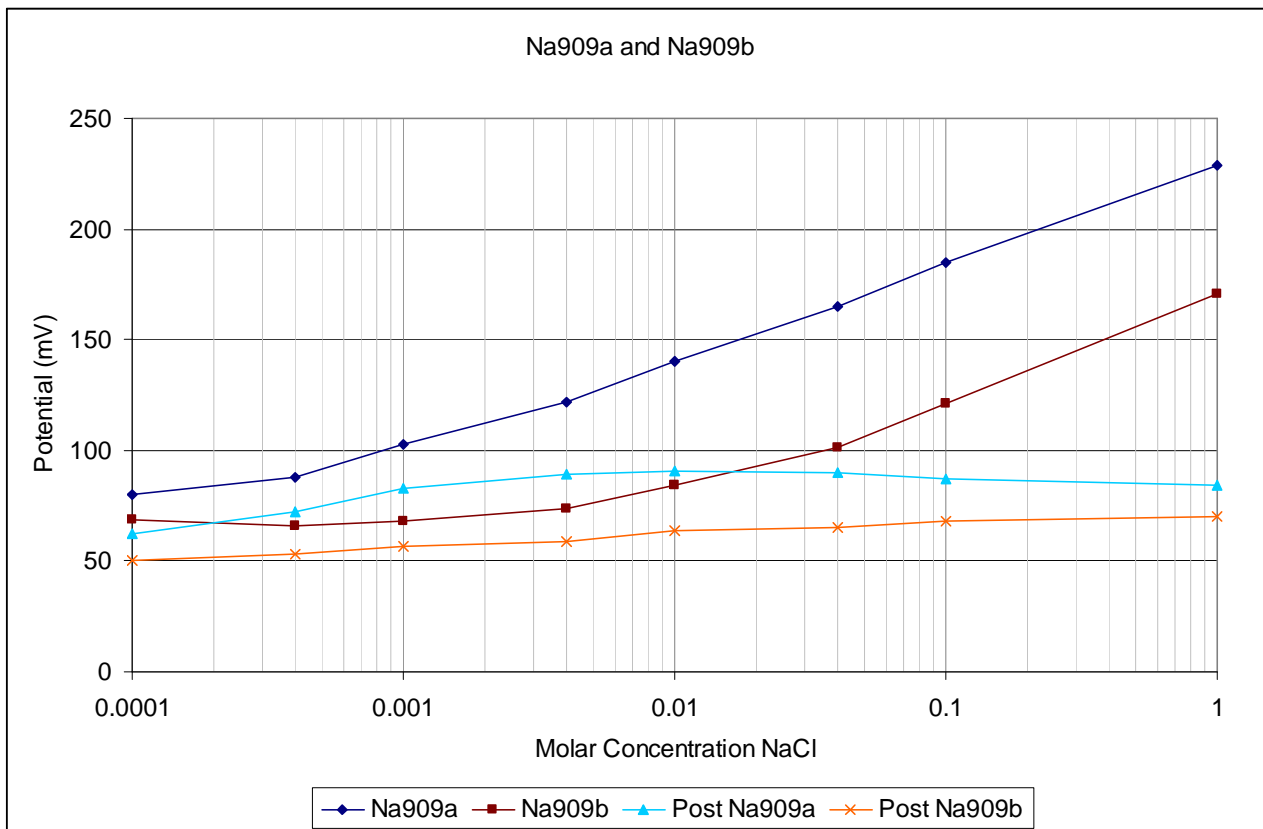


*Note: the pre-test and the post-test curves represent the calibration of the sensor before and after (respectively) a four-day laboratory stabilization test. In this case the response of the sensor was better after the four-day test than it was before.*

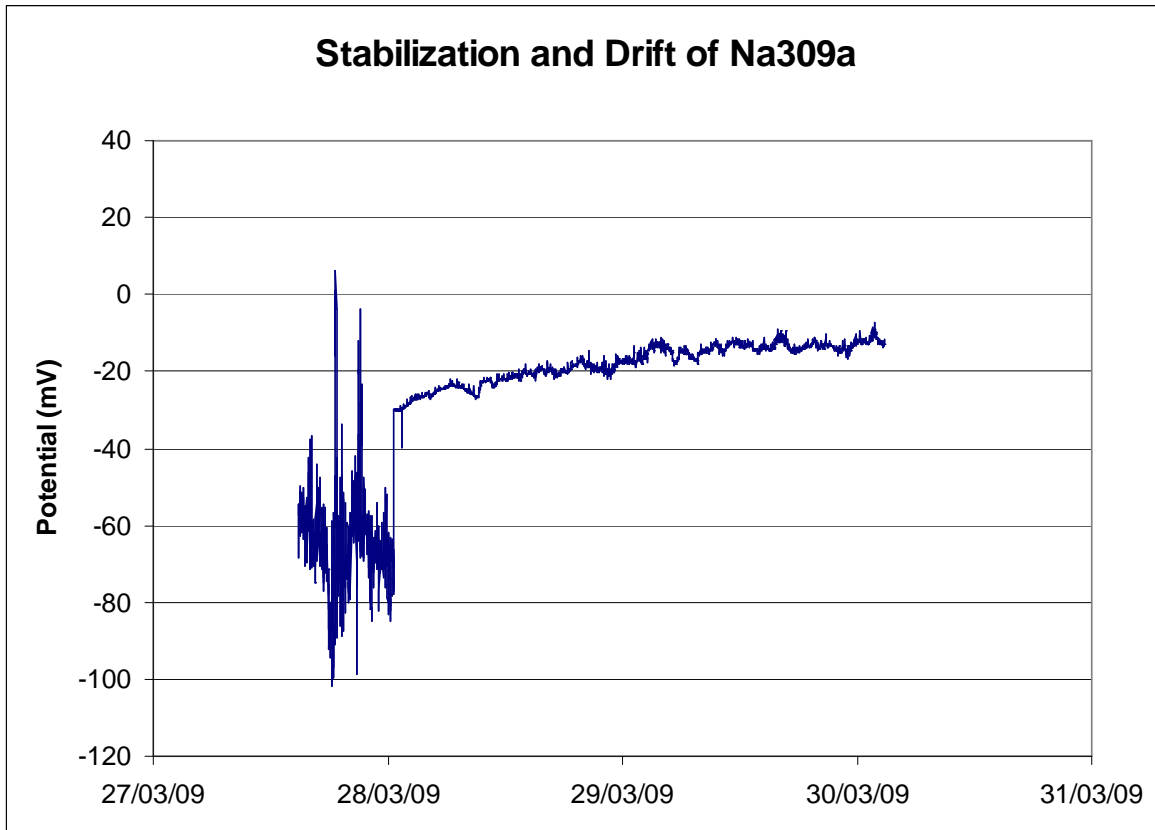




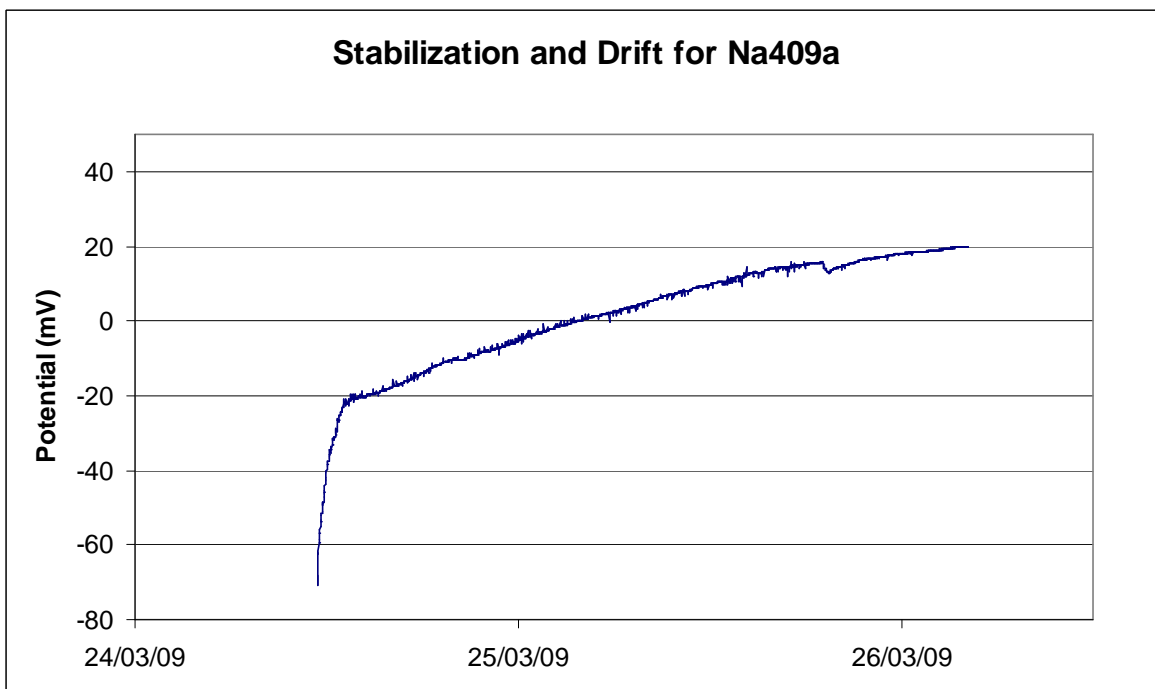


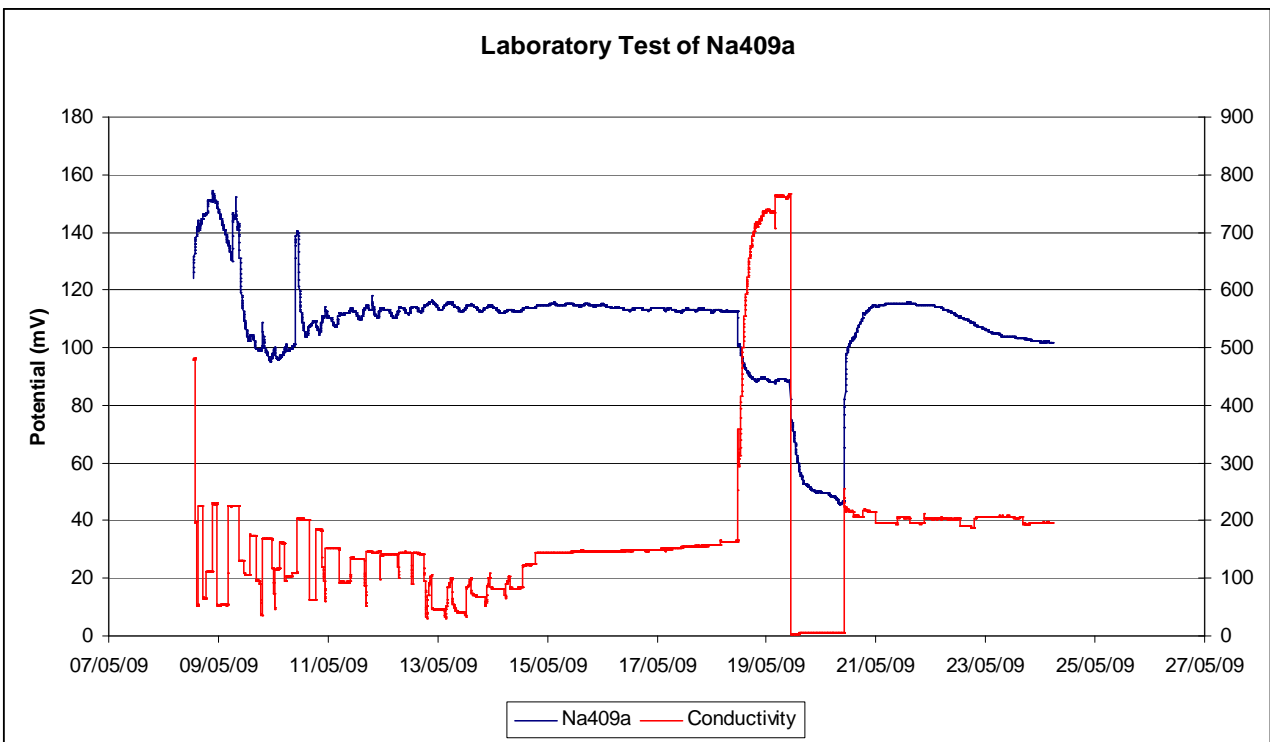
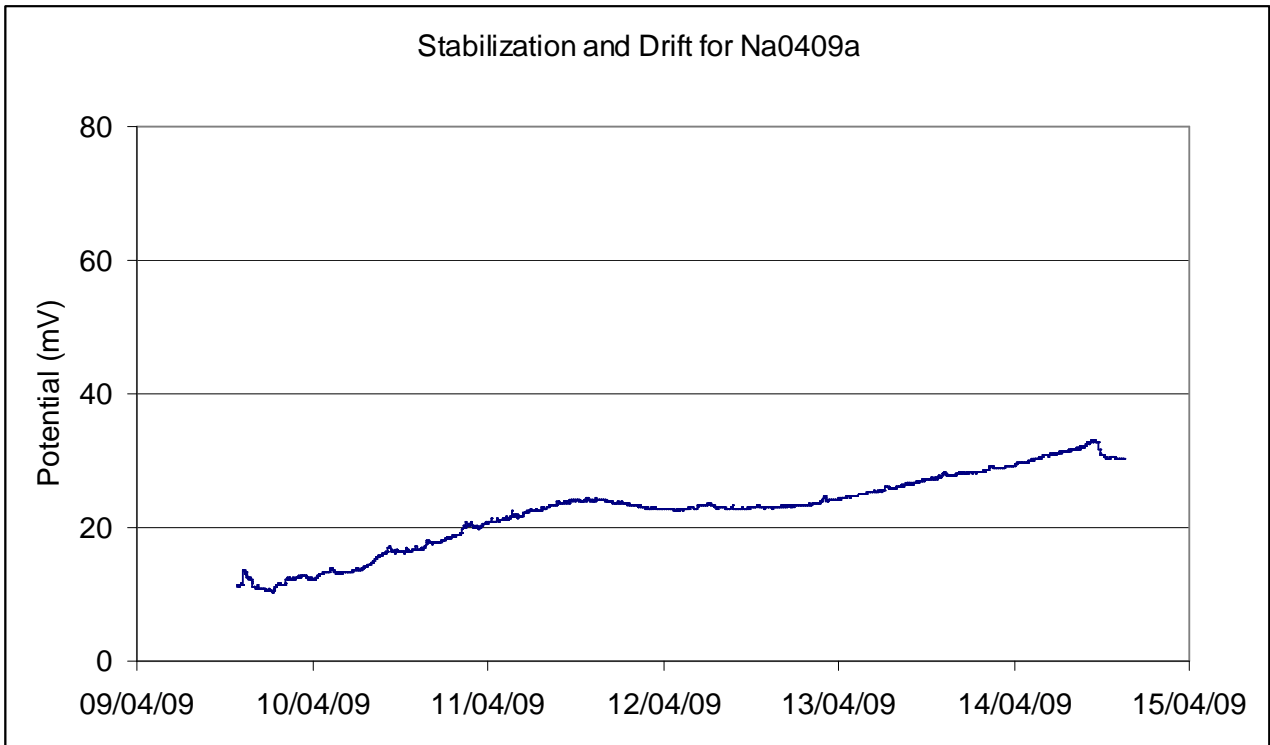


B3.2 Stabilization data for the PVC sensors where long-term testing was conducted.

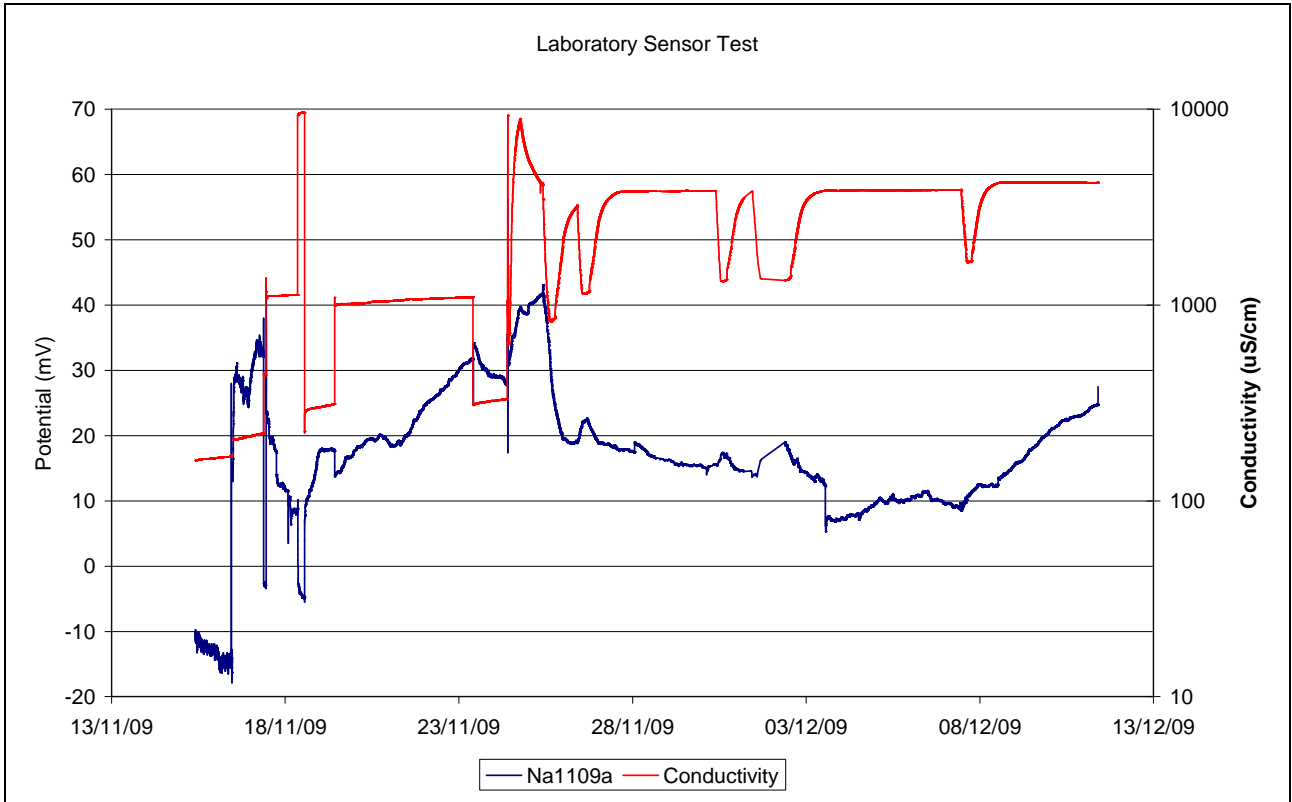


*Note: in the test of Na309a, the first day there was a loose contact, creating the unstable response. The contact was fixed, where the signal became stable again.*





*Note: the test was conducted in changing NaCl concentrations, which are seen in the conductivity response. On the positive change from the 18<sup>th</sup> of May, 2009, the sensor responded opposite of what it should have, where as on the 19<sup>th</sup> and 20<sup>th</sup>, it responded in correctly, just that the size of the response was not in proportion, where it should have been larger on the 19<sup>th</sup> than the 20<sup>th</sup>.*



*Note: the test was conducted in changing NaCl concentrations. The sensor, though very unstable, had a response to the changing concentration as late as November 25, where after it was completely unresponsive to any change.*